Fe
0.4 C
1 Cr
0.2 Mo

4140

1 **GENERAL**

This heat treatable low-alloy steel is similar in chemical composition to Type 4130, except that 4140 has higher carbon content. The increased carbon content provides greater hardenability and strength with some sacrifice in formability and weldability. It is generally used in the oil-quenched and tempered condition, which provides optimum properties; nevertheless, the somewhat lower mechanical properties of the normalized and normalized-and-tempered conditions are adequate for some applications. It can be used to a maximum temperature of about 900 F, above which its strength decreases rapidly with increasing temperature. Like other martensitic and ferritic steels, Type 4140 undergoes a transition from ductile to brittle behavior at low temperatures, the temperature level varying with heat treatment and degree of stress concentration. Since it is susceptible to rusting, it should be protected by paint, electroplate, or other protective coatings for applications in moist, marine, or other corrosive environments. It is widely used in applications requiring a good combination of moderate hardenability, strength, and toughness.

1.01 **Commercial Designation**

4140.

1.02 **Alternate Designations**

AISI 4140, SAE 4140, 4140H, UNS G41400, and UNS J14046.

1.021 The 4140H designation indicates that the steel is made within strict hardenability limits.

1.03 **Specifications**

1.031 Specifications, Table 1.031.

1.04 **Composition**

1.041 Composition, Table 1.041.

1.05 **Heat Treatment**

1.051 Normalize: 1550 to 1650 F, air cool (2, 32).

1.052 Anneal: 1450 to 1600 F, furnace cool (2, 16, 32).

1.053 Harden: 1525 to 1600 F, oil quench. (For water quench, which is rarely used for 4140, 1500 to 1550 F) (2, 32).

1.054 Temper: 350 to 450 F or 700 to 1250 F, 1/2 hour minimum, air cool or water quench. Tempering in the range 450 to 700 F is usually not recommended because the blue-brittleness phenomenon occurs in that range. The alloy is not susceptible to temper embrittlement which occurs in some low-alloy steels in the range 800 to 1100 F (2).

1.055 Spheroidize: 1400 to 1425 F, 6 to 12 hours, furnace cool (2), or 1550 F, furnace cool to 1300 to 1350 F, 6 hours, air cool (16).

1.056 Stress relieve: 1100 to 1250 F, air cool.

1.06 **Hardness**

1.061 Effect of tempering temperature on hardness, Figure 1.061.

1.062 Effect of diameter on surface hardness of quenched and tempered bar, Figure 1.062.

1.063 Effect of diameter on as-quenched hardness at various locations on cross section of bar, Figure 1.063.

1.064 Effects on room temperature hardness of exposures up to 30 hours at various elevated temperatures, Figure 1.064.

1.065 Hardness in unhardened conditions, Table 1.065.

1.066 Effects of 1-hour exposures to elevated temperatures on the room temperature hardness of bars cold rolled various amounts after heat treatment, Figure 1.066.

1.067 Effects of 1-hour exposures to elevated temperatures on the room temperature hardness of bars that had been annealed and then cold rolled various amounts, Figure 1.067.

1.068 End-quench hardenability, Figure 1.068.

1.069 Increased phosphorus (within the specified composition limit) increases the hardenability of Type 4140, as shown in Figure 1.0610. This behavior is attributed to segregation and interaction of phosphorus and carbon at austenite grain boundaries (43).

1.0610 End-quench hardenability curves for 4140 containing high and low phosphorus, Figure 1.0610.

1.07 **Forms and Conditions Available**

1.071 Wrought products are available in the full range of sizes and forms including plate, sheet, strip, bars, rods, billets, forgings, and tubing. The products can be furnished in the annealed, normalized, spheroidized hot-finished, cold-finished, die-drawn-and-tempered, and hardened-and-tempered conditions (1, 2, 16)

1.072 Sand, centrifugal, and investment castings are available in all heat treated conditions.

1.08 **Melting and Casting Practice**

1.081 The alloy is generally air melted in basic-electric, basic-open-hearth, or basic-oxygen furnaces. For some applications requiring exceptional quality, it is induction or consumable-electrode remelted in vacuum.

1.09 **Special Considerations**

1.091 Most of the common acid-pickling processes can cause hydrogen embrittlement of Type 4140 that has been heat treated to high strength levels. However, nitric acid has been reported to be hydrogen embrittling only when used in the range 0.3 to 0.8N. Higher concentrations are recommended for pickling purposes. Anodic cleaning processes are nonhydrogen embrittling because the workpiece is made the anode during electrolysis; consequently, no hydrogen is deposited on it. Alkaline descaling has also been reported to provide complete freedom from hydrogen embrittlement. Hydrogen embrittlement resulting from acid pickling can generally be relieved by baking about 2 to 4 hours at 375 F (15).

1.092 Cadmium plating and chromium plating can induce hydrogen embrittlement in Type 4140 that has been heat treated to tensile strength levels above 180 ksi. Ductility can be restored by baking at 375 F for 4 hours after cadmium plating and for 2 hours after chromium plating (9).

1.093 Hydrogen embrittlement can also occur in Type 4140, heat treated to F_{tu} above 180 ksi, when it is exposed to an environment of high-pressure hydrogen. The embrittlement can be relieved by

Fe
0.4 Cr
1 Cr
0.2 Mo
4140

exposure to air at room temperature for one or more days (8, 14).

1.0931 Effects of exposures to high pressure hydrogen on notched tensile strength, Table 1.0931.

1.094 In commercial wrought grades, transverse mechanical properties are inferior to longitudinal due to inclusions which act as stress raisers with their major effects in the transverse direction. (See Tables 3.0216, 3.0217, and 3.0233 and Figure 3.051.) Available data indicate that this directionality is more pronounced the larger the section size and the higher the strength. It can be minimized by vacuum melting or any other means of reducing nonmetallic inclusions (29).

1.095 Studies of Type 4140 castings have shown that gas holes and shrinkage defects cause percentage decreases in tensile strength appreciably greater than the percentage of cross section that they occupy (3).

1.0951 Effect of gas holes and shrinkage defects on tensile strength of castings, Figure 1.0951.

1.096 Type 4140 is subject to stress corrosion and to corrosion fatigue, especially when heat treated to high hardness levels. Crack propagation rates are increased and fatigue strength is considerably reduced in aqueous or seawater environments. (See Section 2.031.)

1.097 Type 4140 is embrittled at intermediate temperatures when in contact with lead, cadmium, or other low melting point metals. Type 4140 to which lead has been added for improved machinability and Type 4140 which has been cadmium plated for improved corrosion resistance are not suitable for use above 450 F. (See Sections 2.033 and 3.0315.)

2 PHYSICAL PROPERTIES AND ENVIRONMENTAL EFFECTS

2.01 Thermal Properties

2.011 Melting range, about 2790 F.

2.012 Phase changes.

2.0121 Time-temperature-transformation diagram, Figure 2.0121.

2.0122 Upon heating under equilibrium conditions, transformation from pearlite or martensite to austenite starts at 1380 F (Ac1) and is complete at 1460 F (Ac3) (2).

2.0123 Upon slow cooling under equilibrium conditions, the transformation from austenite to pearlite starts at 1370 F (Ar3) and is complete at 1280 F (Ar1) (2).

2.0124 Upon rapid quenching from the austenitic condition the transformation to martensite starts at 650 F (Ms) and is complete at 500 F (Mf) (2).

2.013 Thermal conductivity, 22 Btu ft/hr ft^2 F (34).

2.014 Thermal expansion, 6.3 x 10^{-6} in./in./F from 0 to 200 F (34).

2.015 Specific heat, 0.107 Btu/lb F (34).

2.016 Thermal diffusivity.

2.02 Other Physical Properties

2.021 Density, 0.283 lb/$in.^3$, 7.83 gr/cm^3 (34).

2.022 Electrical properties.

2.023 Magnetic properties, ferromagnetic.

2.024 Emittance.

2.025 Damping capacity.

2.03 Chemical Environments

2.031 Stress corrosion.

2.0311 Type 4140 heat treated to high strength levels is subject to stress corrosion cracking in aqueous environments, including distilled water. Hardness or strength level is the primary criterion for assessing susceptibility to stress corrosion. As shown in Figure 2.0312, the critical hardness level for stress corrosion cracking in boiling distilled water is 40 to 42 HRC, corresponding to a yield strength of 170 to 185 ksi. Harder material failed in a matter of hours under the conditions shown, while softer material did not fail after 200 hours' exposure. Similar behavior may be expected at room temperature at longer times. This critical hardness level is confirmed by laboratory tests, atmospheric service tests, and practical experience.

Type 4140 steel at all hardness levels fails more readily by stress corrosion cracking in nitrate solutions than in distilled water or in aqueous sodium chloride solutions. Stress corrosion cracking in nitrate solutions is attributed to reduction in metal bond strength by NO_3^- ions adsorbed on appropriate imperfection sites associated with carbon atoms. At higher hardness levels, adsorbed water alone reduces metal bond strength sufficiently to initiate cracks (44, 45). (See also Table 3.0281.)

2.0312 Effect of heat treated hardness on stress corrosion cracking in aqueous solutions, Figure 2.0312.

2.0313 The resistance to stress corrosion cracking is improved by cold work, as shown in Figure 2.0314.

2.0314 Effect of cold rolling on stress corrosion cracking in boiling aqueous solutions, Figure 2.0314.

2.0315 A thin decarburized soft surface layer over a core of hardness greater than HRC 40 effectively prevents initiation of stress corrosion cracking (45).

2.0316 The stress corrosion crack-growth rate is faster in distilled water than in air, as shown in Figure 2.0317.

2.0317 Stress corrosion crack-growth rate as a function of stress intensity in water and in air at room temperature, Figure 2.0317.

2.0318 The fatigue strength is considerably reduced in seawater as compared to air because of corrosion fatigue, as shown in Figure 2.0319.

2.0319 Corrosion fatigue in natural seawater as compared to air at room temperature, Figure 2.0319.

2.032 Oxidation.

2.0321 Type 4140 will ignite and burn when fractured in 1000 psig oxygen flowing at 1400 fps at a nominal temperature of about 600 F. The ignition temperature increases as the oxygen pressure is reduced (46).

2.033 Metal-induced embrittlement.

2.0331 Although wrought 4140 steel is normally ductile, embrittlement and delayed fracture can result when the alloy is placed under tensile stress and simultaneously into intimate contact with certain lower-melting metals. This phenomenon, termed metal-induced embrittlement, has been observed with solid cadmium, lead, tin, zinc, and solid and liquid indium (47); it is very similar to the tensile embrittlement discussed later in Section 3.0315.

The lowered fracture stress can be lower than the normal yield stress. Delayed fracture can be separated into two component processes, crack initiation and crack propagation. The temperature dependence of the time required for each of these two processes is shown in Figure 2.0332 for 4140 steel coated with indium in the center of the reduced section of tensile specimens. Crack initiation occurs after an incubation period of minutes to hours below the melting point of indium and after minutes or fractions of a minute above the melting point. This process is stress dependent and occurs more rapidly with increasing stress above a threshold stress of 150 ksi at temperatures near the melting point of indium. Crack propagation time, however, is independent of stress. It is temperature dependent below the melting point of indium, but occurs almost instantaneously above the melting point. The time for crack initiation is believed dependent on diffusion of indium along grain boundaries of the 4140 steel. Crack propagation depends on the presence of indium at the advancing crack tip, which is governed by indium self-diffusion in the solid state or liquid metal flow in the liquid state (47, 48).

2.0332 Delayed fracture of 4140 steel caused by metal-induced embrittlement with indium [(a) crack initiation and (b) crack propagation], Figure 2.0332.

2.04 **Nuclear Environments**

3 MECHANICAL PROPERTIES

3.01 **Specified Mechanical Properties**

3.011 AMS specified mechanical properties at room temperature, Table 3.011.

3.02 **Mechanical Properties at Room Temperature**

3.021 Tension – stress-strain diagrams – tension properties.

3.0211 Effect of tempering temperature on tensile properties of bar, Figure 3.0211.

3.0212 Effect of tempering temperature on tensile properties of castings, Figure 3.0212.

3.0213 Effect of diameter on tensile properties of quenched and tempered bar, Figure 3.0213.

3.0214 Tensile properties of normalized bars from 1/2 to 4 inch in diameter and of annealed bar 1.0 inch in diameter, Figure 3.0214.

3.0215 Effect of cold rolling on tensile properties of bar, Figure 3.0215.

3.0216 Tensile properties of extrusions, Figure 3.0216.

3.0217 Effect of specimen orientation on tensile properties of 6-inch-diameter bar heat treated to two hardness levels, Figure 3.0217.

3.0218 Tensile properties of bar in unhardened conditions, Table 3.0218.

3.0219 Tensile properties of castings, Table 3.0219.

3.02110 Relation between yield strength and hardness for 4140 steel, Figure 3.02110.

3.02111 The ultimate tensile strength of 4140 steel varies with carbide particle size and shape as shown in Figure 3.02112. Carbides in as-quenched material or in material tempered at 390 F or 570 F are needle-shaped, while those produced by tempering at 1020 F or higher are spheroidal. The latter carbides are larger and less strengthening than the former. The spheroidal carbides reflect diffusional coarsening and the reduction of total surface energy as compared to newly precipitated needle-shaped carbides (49). The ultimate tensile strength of as-quenched 4140 steel is approximately equal to the stress for microvoid formation. The initiation of microvoids, either by decohesion at the carbide/matrix interface or by cracking of the carbides themselves, may be the critical stage in the ductile fracture process (50).

Fe
0.4 C
1 Cr
0.2 Mo

4140

3.02112 Variation of ultimate tensile strength with carbide size and shape, Figure 3.02112.

3.02113 The monotonic and cyclic stress-strain curves for as-quenched material and for material tempered at 390, 750, and 1200 F (determined by the incremental step test) are shown in Figure 3.02114. Cyclic hardening is exhibited in the as-quenched condition, while the tempered materials all show cyclic softening. Cyclic softening is at a maximum for material tempered at 750 F. This softening is attributed to (a) mechanical "unpinning" of dislocations and (b) reduction in internal stress through generation of a fatigue substructure. Both the monotonic and cyclic stress-strain curves show a stress-differential effect, with compressive flow stresses being higher than the tensile flow stresses (51).

3.02114 Monotonic and cyclic true stress-true strain curves for 4140 steel [(a) austenitized and quenched, (b) tempered at 390 F, (c) tempered at 750 F, and (d) tempered at 1200 F], Figure 3.02114.

3.022 Compression – stress-strain diagrams – compression properties. (See also Section 3.02113.)

3.0221 Compressive yield strength. (See Figure 3.0321.)

3.023 Impact.

3.0231 Effect of tempering temperature on impact properties at room temperature, Figure 3.0231.

3.0232 Transverse impact properties of leaded and non-leaded 6-inch-diameter bar at room temperature, Figure 3.0232.

3.0233 Impact properties of extruded bar at room temperature in various heat treated conditions, Table 3.0233.

3.024 Bending.

3.025 Torsion and shear (see Figure 3.0351).

3.0251 Effect of tempering temperature on torsional properties, Figure 3.0251.

3.026 Bearing (see Figure 3.0361).

3.027 Stress concentration.

3.0271 Notch properties (see Table 1.0931).

3.0272 Fracture toughness.

3.02721 Effect of quenching and tempering temperature on plane strain fracture toughness, Figure 3.02721.

3.028 Combined properties.

3.0281 Burst properties of small pressure vessels, Table 3.0281.

3.03 **Mechanical Properties at Various Temperatures**

3.031 Tension – stress-strain diagrams – tension properties.

3.0311 Effect of elevated temperatures on tensile properties of quenched and tempered bar, Figure 3.0311.

Fe
0.4 Cr
1 Cr
0.2 Mo

4140

3.0312 Effect of exposure time at test temperature on elevated temperature tensile properties, Figure 3.0312.

3.0313 Effects of temperatures from -100 F to 200 F on tensile properties, Figure 3.0313.

3.0314 Effects of temperatures from -200 F to 80 F on tensile properties of 4140 tempered at 1050 F and at 725 F [(a) tempered at 1050 F, and (b) tempered at 725 F], Figure 3.0314.

3.0315 Type 4140 is embrittled during tensile testing at intermediate temperatures (roughly 400 F to 900 F) when in intimate contact with lead, cadmium, zinc, tin, or indium. The embrittling agent can be present internally, such as leaded 4140 for improved machinability, or on the surface, such as cadmium electroplated 4140 for improved corrosion resistance. Embrittlement becomes apparent above about 0.75 of the melting point of the low melting metal and is recovered at some temperature above this melting point. Tensile data for Type 4140 externally wetted with high purity lead are compared in Figure 3.0316 with similar data for clean Type 4140. Above about 350 F, or 0.75 of the absolute melting point of lead (621 F), the reduction in area and true fracture strength are significantly reduced. The effects of solid cadmium, zinc, tin, and indium are similar, with losses of RA noted at temperatures which are relative to the melting points of the respective embrittling metals (52).

External wetting with lead alloys containing small amounts of tin, antimony, zinc, or bismuth intensify the severity of embrittlement and/or extend the temperature range of embrittlement as compared to wetting with pure lead. The temperature for ductility recovery ranges from just above the melting point of lead for material wet with high purity lead to above 900 F for material wet with Pb-25Bi or Pb-0.1Zn (53).

Embrittlement is associated with the presence of the low melting metal at the crack tip during deformation of 4140. At temperatures above the melting point, the embrittling metal is believed to proceed down the crack as a liquid, aided by surface tension effects, and to complete its path to the crack tip as a vapor. At temperatures below the melting point, it has been proposed that the transit is by vapor transport alone (54), in contrast to the diffusional mechanism proposed for metal-induced embrittlement (47). (See Section 2.033.)

3.0316 Effects of surface wetting with lead on tensile properties [(a) unwetted and (b) wetted with pure lead], Figure 3.0316.

3.0317 The susceptibility to lead embrittlement can be reduced by prior cold work, as shown in Figure 3.0318. The entire embrittlement trough, which extends from 400 F to 850 F, can virtually be eliminated by combining cold work with heat treatment to produce material with the desired tensile strength, in this case 200 ksi. The room temperature ductility, however, is reduced by cold work. A second technique for elimination of lead embrittlement involves rare earth alloying through the addition of mischmetal during melting. In this case, cerium associates with the lead and eliminates embrittlement, as shown in Figure 3.0319 (54).

3.0318 Elimination of lead embrittlement by prior cold deformation, Figure 3.0318.

3.0319 Elimination of lead embrittlement by the addition of rare earth elements, Figure 3.0319.

3.032 Compression -- stress-strain diagrams -- compression properties.

3.0321 Effect of temperature on compressive yield strength of bar and forgings heat treated to various strength levels, Figure 3.0321.

3.033 Impact.

3.0331 Effects of test temperature, tempering temperature, and percentage of martensite in microstructure on impact properties, Figure 3.0331.

3.0332 Effects of exposures up to 30 hours at various elevated temperatures on impact resistance at -40 F, Figure 3.0332.

3.0333 Effects of temperature and prestrain on impact resistance of annealed bar, Figure 3.0333.

3.0334 Impact properties of castings at 70 F and -50 F, Table 3.0334.

3.0335 Effects of temperature from -200 F to 80 F on impact energy of 4140 tempered at 1050 F and at 725 F, Figure 3.0335.

3.0336 Effect of tempering temperature on impact resistance at -40 F, Figure 3.0336.

3.0337 Effect of tempering temperature on impact ductile-brittle transition temperature, Figure 3.0337.

3.034 Bending.

3.035 Torsion and shear.

3.0351 Effect of temperature on shear strength of bar and forgings heat treated to various strength levels, Figure 3.0351.

3.0352 Effects of temperature from -200 F to 80 F on shear strength of 4140 tempered at 1050 F and at 725 F, Figure 3.0352.

3.036 Bearing.

3.0361 Effect of temperature on bearing strength of bar and forgings heat treated to various strength levels, Figure 3.0361.

3.037 Stress concentration.

3.0371 Notch properties.

3.03711 Effects of temperature from -200 F to 80 F on notched/unnotched tensile strength ratio of 4140 tempered at 1050 F and at 725 F, Figure 3.03711.

3.0372 Fracture toughness.

3.03721 A transition in crack arrest fracture toughness at 0 F is observed for 4140 tempered to 160 ksi or 180 ksi, as shown in Figure 3.03722. This transition appears to be associated with a change in fracture mechanism from cleavage at subtransition temperatures to dimpled rupture at supertransition temperatures (55).

3.03722 Crack arrest fracture toughness of 4140 steel as a function of test temperature, Figure 3.03722.

3.038 Combined properties.

3.04 **Creep and Creep-Rupture Properties**

3.041 Creep properties at 1000 F and 1200 F of sheet in various heat treated conditions, Figure 3.041.

3.042 Effect of cold rolling on creep-rupture time of quenched and tempered rod at various combinations of temperature and stress, Figure 3.042.

3.043 Effect of cold rolling on minimum creep rate of quenched and tempered rod at various combinations of temperature and stress, Figure 3.043.

3.05 **Fatigue Properties**

3.051 Longitudinal and transverse fatigue properties of smooth and notched specimens, Figure 3.051.

3.052 Fatigue properties of smooth bars heat treated to various strength levels, Figure 3.052.

3.053 Fatigue properties of notched bars heat treated to various strength levels, Figure 3.053.

3.054 Effects of decarburization on fatigue properties of smooth and notched specimens, Figure 3.054.

3.055 Fatigue properties of leaded and nonleaded bar at two hardness levels, Figure 3.055.

3.056 Fatigue properties of annealed bar, Figure 3.056.

3.057 Effects of various environments on fatigue properties in different heat treated conditions, Figure 3.057.

3.058 Fatigue data for investment-castings showing improvement in fatigue life and consistency of results produced by machining and sand blasting, Figure 3.058.

3.059 Room temperature fatigue behavior of quenched and tempered 4140 [(a) tempered at 390 F and (b) tempered at 1200 F], Figure 3.059.

3.0510 Effects of notches on cyclic fatigue life at room temperature, Figure 3.0510.

3.0511 Tempering after quenching from 1830 F reduces the room temperature fatigue crack-growth rate, as shown in Figure 3.0512. Lowest crack-growth rates are observed for material tempered at 750 F to 1200 F. Crack-growth rates after tempering are higher in compression-tension fatigue (R = -1) than in zero-tension fatigue (R = 0) for the 970 F and 1230 F tempers, as shown in Figure 3.0513. The threshold stress for fatigue crack propagation in quenched and tempered alloy is approximately 3.6 ksi$\sqrt{\text{inch}}$, as shown in Figure 3.0514.

3.0512 Room temperature fatigue crack-growth behavior of 4140 steel austenitized at 1830 F and tempered at 390 F to 1200 F, Figure 3.0512.

3.0513 Room temperature fatigue crack-growth behavior of 4140 steel austenitized at 1550 F and tempered at 720 F to 1550 F [(a) R = 0, and (b) R = -1], Figure 3.0513.

3.0514 Room temperature fatigue crack-growth behavior of quenched and tempered 4140 steel at low stresses, Figure 3.0514.

3.06 **Elastic Properties**

Elastic properties are generally assumed to be equivalent to those of Type 4130, Code 1201.

3.061 Poisson's ratio.

3.062 Modulus of elasticity.

3.063 Modulus of rigidity.

3.064 Tangent modulus.

3.065 Secant modulus.

4 FABRICATION

4.01 **Forming**

4.011 Type 4140 can be cold formed to a reasonable extent in the annealed condition, but its cold formability is somewhat inferior to that of Type 4130, Code 1201.

4.012 4140 has good hot workability. Forging should be carried out within the range 2200 F to 1700 F, the optimum range being 2200 F to 2000 F. Hot rolling should be started in the range 2250 F to 2350 F. Parts should be cooled slowly after hot forming (2, 16).

	Fe
0.4	C
1	Cr
0.2	Mo

4140

4.02 **Machining and Grinding**

4.021 Type 4140 has good machinability in the annealed and cold drawn conditions. Cold drawn material has a machinability rating of 62 percent of AISI B1112 Bessemer screw stock. When annealed prior to cold drawing, the machinability rating advances about 10 percent for most machining operations. The leaded grade has appreciably better machinability than the standard grade (2).

4.03 **Joining**

4.031 This alloy can be readily welded by any of the manual or automatic electric-arc techniques. Low-hydrogen electrodes of the appropriate strength level are recommended. Since there is danger of embrittlement in the heat-affected zone, preheating is required and postweld heat treating may be necessary depending on the application. If postweld heat treating is not done, preheat and interpass temperature of 600 F minimum, followed by slow cooling, is recommended. If postweld heat treating is done, preheat and interpass temperature of 400 F minimum is suggested, followed by transfer of weldment into furnace immediately after welding for postweld heat treatment at 1100 F to 1250 F, followed by slow cooling. If the postweld treatment cannot be done immediately after welding, the weldment should be heated to 600 F immediately following welding, held at temperature 1 hour per inch of thickness, slow cooled to ambient temperature and then subsequently postweld heat treated (2, 16).

4.04 **Surface Treating**

4.041 With proper surface preparation, protective coatings of paint and electroplate can be applied with excellent results.

4.042 Type 4140 can be nitrided by gas, salt-bath, or ion-bombardment techniques for improved surface hardness, wear resistance, and fatigue strength. Hardness curves for gas-nitrided and ion-nitrided materials are shown in Figures 4.0421 and 4.0422, respectively. The surface layer generally consists of internal nitrides of alloying elements plus a thin surface layer (termed "white layer") and intergranular network of iron nitride. The presence of iron nitride promotes greater surface hardness and wear resistance but is detrimental to ductility. Fatigue resistance is enhanced by the internal diffusion layer of nitrides of the alloying elements. Anhydrous ammonia is employed as the nitrogen source, with excess hydrogen added to control the nitrogen activity and amount of iron nitride formed. Nitriding times are reduced for ion-nitriding as compared to gas-nitriding (26, 27, 56, 57, 58)

4.0421 Case hardness of alloy nitrided after it had been quenched and tempered at various temperatures, Figure 4.0421.

Fe
0.4 Cr
1 Cr
0.2 Mo

4140

4.0422 Hardness gradient near surface of ion-nitrided 4140 steel, Figure 4.0422.

4.043 Type 4140 can also be surface hardened by laser heat treatment. Surface hardness can be increased from 20 HRC, corresponding to the normalized or annealed condition, to as high as 59 HRC, corresponding to a martensite content of 95 to 100 percent by laser heating a thin surface layer and air quenching (59).

REFERENCES

1 "Modern Steels and Their Properties", Seventh Edition, Handbook 2757, Bethlehem Steel Corp. (1972).

2 "AISI 4140", Alloy Digest, Filing Code: SA-18 (May 1954).

3 Bramfitt, B. L., and Luizzi, L., "A Study of the Effect of Solidification Imperfections on the Tensile Properties of Cast Steel", Benet R & E Labs, Watervliet Arsenal, WVT-6420 (September 1964).

4 DeFries, R. S., "The Elevated Temperature Properties of Two 81MM Mortar Tube Alloys 4337M and 4140", Benet R & E Labs, Watervliet Arsenal, WVT-7106 (June 1971).

5 Thorkildsen, R. L., "High-Temperature Materials Program", Materials Technology Inc., MTI 65TR45 (September 2, 1965).

6 Larson, F. R., "The Effect of Microstructure on the Impact Properties of Some Commercial Alloy Steels With and Without Boron", Watertown Arsenal, WAL TR 310/215 (April 1958).

7 "Fatigue Properties of Investment Castings", U.S. Army Weapons Command, Technical Report RE-71-2 (April 1971).

8 Owens, W. H., "The Effect of High-Pressure Hydrogen on SAE 4140 and 1018 Steels at Ambient Temperatures", Aro, Inc., AEDC-TR-66-269 (December 1977).

9 "Methods for Minimizing the Embrittling Effect of Hydrogen in Electroplated High Strength Alloy Steel Items", Frankfort Arsenal, IEP 60-6110-2 (March 1963).

10 "Mechanical Tests on Various Extruded Materials", Allegheny-Ludlum Steel Corp. (January 1, 1956).

11 Romine, H. E., "Correlation of Laboratory Fracture Toughness Tests With Burst Tests of Thin-Wall Steel Pressure Vessels Containing a 2t Through-Crack Flaw", Naval Weapons Lab, NWL Technical Report TR-2270 (March 1969).

12 "Atlas of Isothermal Transformation Diagrams", U.S. Steel Corp. (1951).

13 SAE Handbook, 1972 Edition.

14 Cataldo, C. E., "Compatibility of Metals With Hydrogen", Geo. C. Marshall Space Flight Center, NASA TM X-53807 (December 26, 1968).

15 Groeneveld, T. P., Fletcher, E. E., and Elsea, A. R., "A Review of the Literature on Cleaning, Pickling, and Electroplating Processes and Relief Treatments to Minimize Hydrogen Embrittlement of Ultrahigh-Strength Steels", Battelle Memorial Institute, Contract NAS8-20029 (October 15, 1966).

16 "Steels for Elevated Temperature Service", U.S. Steel Corp. (June 1972).

17 AMS 5338C (October 1, 1982).

18 AMS 6378C (April 1, 1983).

19 AMS 6381C (May 15, 1972).

20 AMS 6382J (July 1, 1981).

21 AMS 6390B (July 1, 1976).

22 AMS 6395B (October 15, 1979).

23 "Cross-Index of Chemically Similar Specifications and Identification Code", MIL-HDBK-H1D (June 22, 1970).

24 Metals Handbook, 8th Edition, ASM (1961).

25 Lee, R. H., and Uhlig, H. H., "Corrosion Fatigue of Type 4140 High-Strength Steel", *Metallurgical Transactions*, Vol. 3 (November 1972), pp 2949–2957.

26 Schwartzkopf, A. J., "New Facts on the Nitriding of 4140 and 4340", *Iron Age*, Vol. 181 (May 29, 1958), pp 90–93.

27 Boempler, D., "The Load Carrying Capacity of Bath Nitrided Gears", American Gear Manufacturers Institute, AGMA 109.18 (October 1966).

28 Simmons, W. F., and Cross, H. C., "Elevated-Temperature Properties of Wrought Medium-Carbon Alloy Steels", *ASTM STP*, No. 199 (1957).

29 Simon, W., "Fatigue, Impact, and Tensile Properties of High-Strength Leaded and Non-Leaded SAE 4140 Steel", SAE Transactions, Vol. 69 (1961), pp 69–76.

30 Evans, E. B., Ebert, L. J., and Briggs, C. W., "Fatigue Properties of Comparable Cast and Wrought Steels", *Proceedings ASTM*, Vol. 56 (1956), pp 979–1009.

31 Jackson, L. R., and Pochapsky, T. E., "The Effect of Composition on the Fatigue Strength of Decarburized Steel", *Transactions ASM*, Vol. 39 (1947), pp 45–57.

32 "Mechanical Properties of Alloy Steel", Republic Steel Corp. (1961).

33 Shahinian, P., Achter, M. R., and Pennington, W. A., "The Effect of Cold Work and Temperature on Strength and Structure of Steel", *Trans. ASM*, Vol. 53 (1961).

34 "Strength of Aircraft Elements", MIL-HDBK-5B (September 1971).

35 "Guide to Steel Selection", Joseph T. Ryerson & Son, Inc., Bulletin No. R-8-6-2.

36 "Haynes Low Alloy Steels", Haynes-Stellite Co. (1959).

37 Fiorentino, R. J., and Sabroff, A. M., "Availability and Mechanical Properties of High-Strength Steel Extrusions", DMIC Report 138 (October 26, 1960).

38 Grobecker, D. W., "Metals for Supersonic Aircraft and Missiles", Proceedings of the Conference on Heat Tolerant Metals for Aerodynamic Applications (January 1957).

39 Steigerwald, E. A., "Plane Strain Fracture Toughness for Handbook Presentation", TRW Inc., AFML TR-67-187 (July 1967). (This publication is subject to export control. Export permitted only with the approval of AFML.)

40 Miller, J., Smith, L. W., and Porter, P. K., "Utilization of Low-Alloy Materials for High-Temperature Service Applications", U.S. Air Force, AF TR-5929 (June 1949).

41 "Nitralloy and Nitriding", The Nitralloy Corp. (1954).

42 Wood, W. E., Parker, E. R., and Zackay, V. F., "An Investigation of Metallurgical Factors Which Affect Fracture Toughness of Ultra High Strength Steels", Army Materials and Mechanics Research Center Report No. AMMRC CTR 73-24 (May 1973).

43 Jacobs, F. A., and Krauss, G., "The Effects of Phosphorus and Carbon on the Hardenability of 41XX Type Steels", *Journal of Heat Treating*, Vol. 2, No. 2 (December 1981), pp 139–146.

44 Uhlig, H. H., "Critical Potentials for Stress Corrosion Cracking (Mechanism of Stress Corrosion Cracking)", Massachusetts Institute of Technology, Final Report ARO 11266.4-MC (April 1975).

45 Asphahani, A., and Uhlig, H. H., "Stress Corrosion Cracking of 4140 High Strength Steel in Aqueous Solutions", *Journal of the Electrochemical Society*, Vol. 122, No. 2 (February 1975), pp 174–179.

46 Bates, C. E., Wren, J. E., Monroe, R., and Pears, C. D., "Ignition and Combustion of Ferrous Metals in High Pressure, High Velocity, Gaseous Oxygen", *Journal of Materials for Energy Systems*, Vol. 1, No. 1 (June 1979), pp 61–76.

47 Gordon, P., "The Mechanisms of Crack Initiation and Crack Propagation in Metal-Induced Embrittlement of Metals. Part II. Theoretical Aspects of Crack Initiation", Illinois Institute of Technology, Final Report N00014-79-C-0580, NSF-DMR 79-08674 (February 1981).

48 Gordon, P., "The Mechanisms of Crack Initiation and Crack Propagation in Metal-Induced Embrittlement of Metals. Part I. Delayed Failure in the Embrittlement of 4140 Steel", Technical Report N00014-79-C-0580, NSF-DMR 79-08674 (December 1980).

49 Lui, M. W., and Le May, I., "Relations Between Tensile Strength and Carbide Size in AISI 4140 Steel", *Metallurgical Transactions*, Vol. 6A, No. 3 (March 1975), pp 583–584.

50 Lui, M. W., and Le May, I., "The Relation Between Ultimate Tensile Strength and Carbide Size in Steel", *Transactions of the ASME, Series H, Journal of Engineering Materials and Technology*, Vol. 98, No. 2 (April 1976), pp 173–179.

51 Thielen, P. N., Fine, M. E., and Fournelle, R. A., "Cyclic Stress Strain Relations and Strain-Controlled Fatigue of 4140 Steel", *Acta Metallurgica*, Vol. 24, No. 1 (January 1976), pp 1–10.

52 Lynn, J. C., Warke, W. R., and Gordon, P., "Solid Metal-Induced Embrittlement of Steel", *Materials Science and Engineering*, Vol. 18, No. 1 (March 1975), pp 51–62.

53 Landow, M., Harsolia, A., and Breyer, N. N., "Liquid Metal Embrittlement of 4145 Steel by Lead Alloys", *Journal of Materials for Energy Systems*, Vol. 2, No. 4 (March 1981), pp 50–59.

54 Breyer, N. N., and Gordon, P., "Lead Induced Brittle Failures of High Strength Steels", Proceedings of the Third International Conference on the Strength of Metals and Alloys, Vol. I, The Microstructure and Design of Alloys, held in Cambridge, England (August 20–25, 1973), Paper 101.

55 Ripling, E. J., Mulherin, J. H., and Crosley, P. B., "Crack Arrest Toughness of Two High Strength Steels (AISI 4140 and AISI 4340)", *Metallurgical Transactions*, Vol. 13A (April 1982), pp 657–664

56 Jindal, P. C., "Ion Nitriding of Steels", *Journal of Vacuum Science and Technology*, Vol. 15, No. 2 (March/April 1978), pp 313–317.

57 Knechtel, H. E., and Podgurski, H. H., "Bright Nitriding in Bell-Type Furnace With Continuous Recirculation of Atmosphere", *Industrial Heating*, Vol. 46, No. 6 (June 1979), pp 12–14, 16.

58 Anonymous, "Ion Nitriding: A Particularly Versatile Case Hardening Process – Part 1: Function of the Method", *Industrial Heating*, Vol. 48, No. 9 (September 1981), pp 24–25, 27, 29.

59 Grotke, G. E., Bruck, G. J., Smith, J. E., and Nurminen, J. I., "A Parametric Study of Surface Transformation Hardening With High-Power Lasers", Westinghouse Research and Development Center, Pittsburgh, Pennsylvania, Report 84-9D4-SURFC-R1 (February 2, 1984).

60 Briggs, A., Airey, R., and Edwards, B. C., "A Double Torsion Fracture Mechanics and Auger Electron Spectroscopy Approach to the Study of Stress Corrosion Cracking in Low Alloy Steels", *Journal of Materials Science*, Vol. 16, No. 1 (January 1981), pp 125–140.

61 Tipton, D. G., "Corrosion Fatigue of High Strength Fastener Materials in Seawater", Laque Center for Corrosion Technology, Incorporated, Wrightsville Beach, North Carolina, NASA CR-174677 (December 1983).

62 DeFries, R. S., "The Estimation of Yield Strength From Hardness Measurements", Watervliet Arsenal, New York, WVT-TN-75051 (August 1975).

63 Montano, J. W., "Low Temperature Mechanical Properties, Fractographic and Metallographic Evaluation of Several Alloy Steels", National Aeronautics and Space Administration, Marshall Space Flight Center, Huntsville, Alabama, NASA TM X-64791 (November 1973).

64 Tauscher, S., and Thornton, P., "Temper Embrittlement in 4140 Seamless Tubing", Army Armament Research and Development Command, Dover, New Jersey, ARLCB-TR-77043 (November 1977).

65 Ripling, E. J., and Crosley, P. B., "Crack Arrest Toughness of 4140, 1340, and 4340 Steel", Materials Research Laboratory, Incorporated, Glenwood, Illinois, MRL-792 (November 1981).

66 Haibach, E., and Matschke, C., "The Concept of Uniform Scatter Bands for Analyzing S-N Curves of Unnotched and Notched Specimens in Structural Steel", Proceedings of a Symposium, Low-Cycle Fatigue and Life Prediction, ASTM-STP-770, Firminy, France (September 23–25, 1980), pp 549–571.

67 Thielen, P. N., and Fine, M. E., "Fatigue Crack Propagation in 4140 Steel", *Metallurgical Transactions*, Vol. 6A, No. 11 (November 1975), pp 2133–2141.

68 Stephens, R. I., Benner, P. H., Mauritzson, G., and Tindall, G. W., "Constant and Variable Amplitude Fatigue Behavior of Eight Steels", *Journal of Testing and Evaluation*, Vol. 7, No. 2 (March 1979), pp 68–81.

69 Kwun, S. I., and Fine, M. E., "Fatigue Microcrack Growth in Tempered HY80, HY130, and 4140 Steels: Threshold and Mid-Delta K Range", *Fatigue of Engineering Materials and Structures*, Vol. 3, No. 4 (1980), pp 367–382.

	Fe
0.4	C
1	Cr
0.2	Mo

4140

Fe
0.4 Cr
1 Cr
0.2 Mo

4140

Alloy	4140
AMS Specification	Product Form
5338C	Castings
6378C	Bars
6381C	Tubing
6382J	Bars, Forgings, Rings
6390B	Tubing
6395B	Sheet, Strip, Plate

TABLE 1.031. SPECIFICATIONS (17–22)

Alloy	4140					
AMS Specifications	5338C		6378C		6381C, 6382J, 6390B, 6395B	
	Percent		Percent		Percent	
Element	Min	Max	Min	Max	Min	Max
Carbon	0.35	0.45	0.39	0.48	0.38	0.43
Chromium	0.80	1.10	0.75	1.20	0.80	1.10
Molybdenum	0.15	0.25	0.15	0.25	0.15	0.25
Manganese	0.75	1.00	0.70	1.10	0.75	1.00
Silicon	–	1.00	0.15	0.35	0.20[a]	0.35
Copper	–	0.35	–	0.35	–	0.35
Nickel	–	0.25	–	0.25	–	0.25
Phosphorus	–	0.04	–	0.040	–	0.025
Sulfur	–	0.04	0.04	0.060	–	0.025
Tellurium	–	–	0.01	0.02	–	–

(a) 0.15 percent silicon minimum for AMS 6382J and 6395B.

TABLE 1.041. COMPOSITION (17–22)

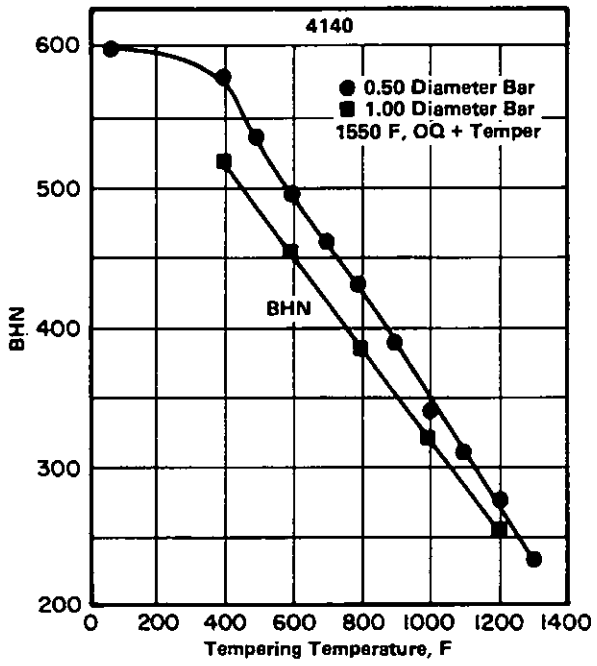

FIGURE 1.061. EFFECT OF TEMPERING TEMPERATURES ON HARDNESS (1, 2)

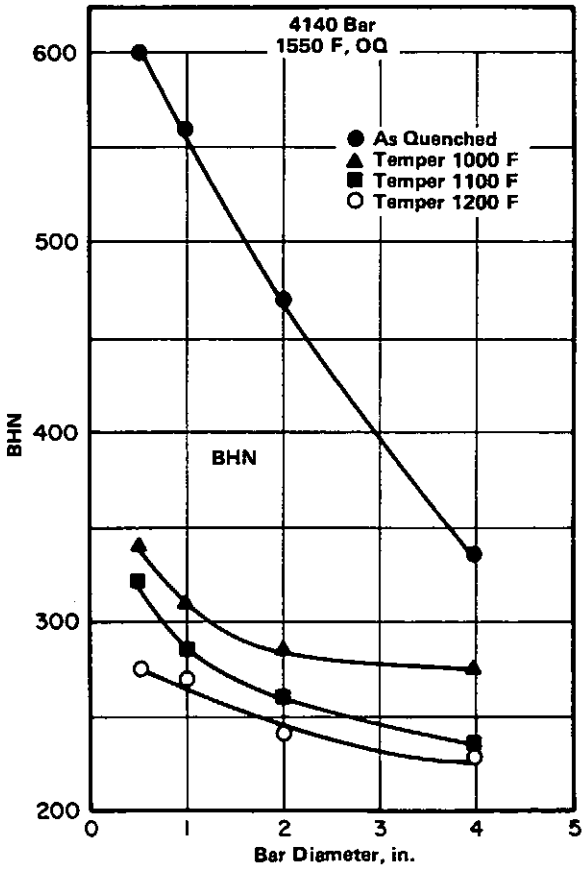

FIGURE 1.062. EFFECT OF DIAMETER ON SURFACE HARDNESS OF QUENCHED AND TEMPERED BAR (1)

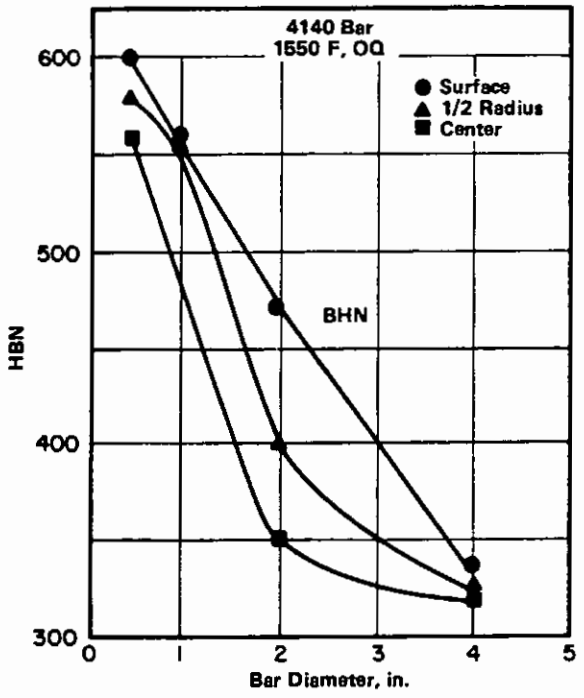

FIGURE 1.063. EFFECT OF DIAMETER ON AS-QUENCHED HARDNESS AT VARIOUS LOCATIONS ON CROSS SECTION OF BAR (1)

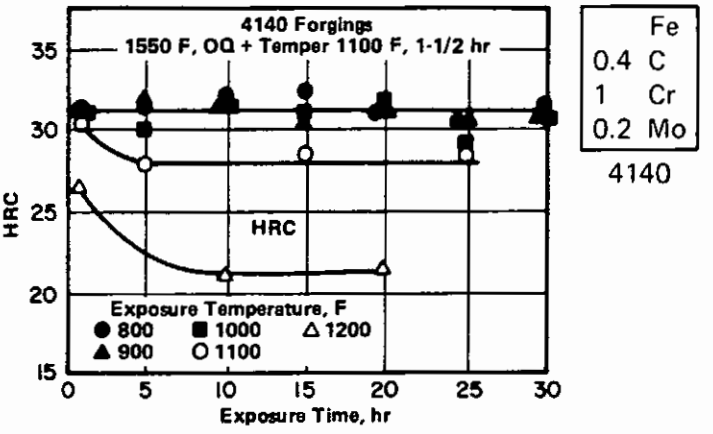

FIGURE 1.064. EFFECTS ON ROOM TEMPERATURE HARDNESS OF EXPOSURES UP TO 30 HOURS AT VARIOUS ELEVATED TEMPERATURES (4)

Alloy	4140	
Condition	Form	BHN
Annealed	1-inch-Diameter Bar	197
	Castings	220
Normalized	1/2-inch-Diameter Bar	302
	1-inch-Diameter Bar	302
	2-inch-Diameter Bar	285
	4-inch-Diameter Bar	241
	Castings	275
Hot Rolled	1-inch-Diameter Bar	229 – 270

TABLE 1.065. HARDNESS IN UNHARDENED CONDITIONS (1, 2)

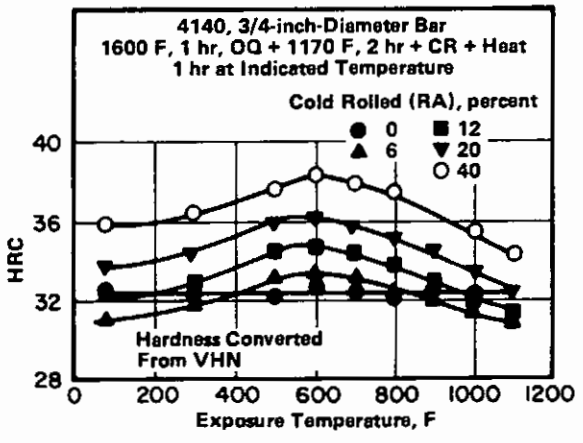

FIGURE 1.066. EFFECTS OF ONE-HOUR EXPOSURES TO ELEVATED TEMPERATURES ON THE ROOM TEMPERATURE HARDNESS OF BARS COLD ROLLED VARIOUS AMOUNTS AFTER HEAT TREATMENT (33)

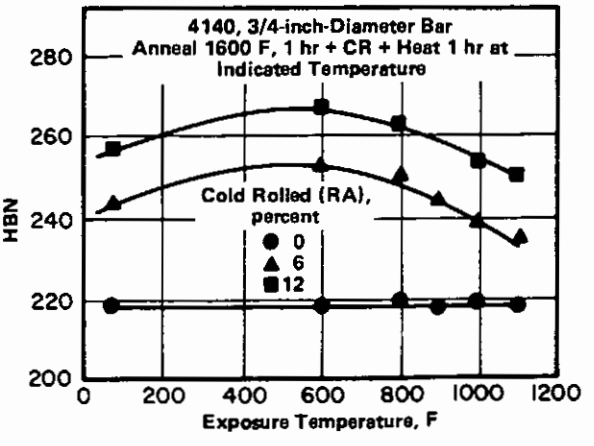

FIGURE 1.067. EFFECTS OF ONE-HOUR EXPOSURES TO ELEVATED TEMPERATURES ON THE ROOM TEMPERATURE HARDNESS OF BARS THAT HAD BEEN ANNEALED AND THEN COLD ROLLED VARIOUS AMOUNTS (33)

Fe
0.4 Cr
1 Cr
0.2 Mo
4140

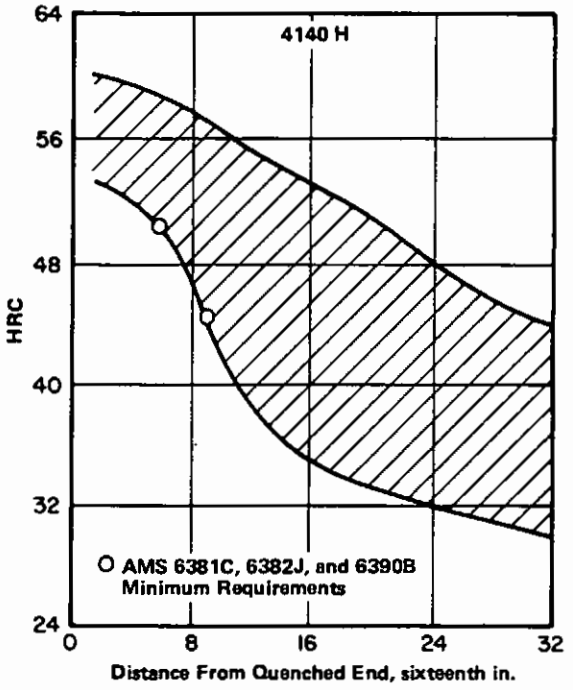

FIGURE 1.068. END-QUENCH HARDENABILITY (13)

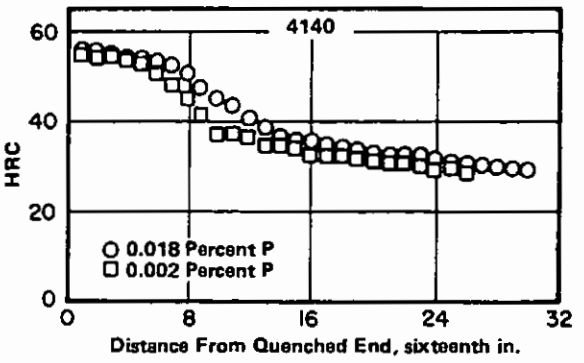

FIGURE 1.0610. END-QUENCH HARDENABILITY CURVES FOR 4140 CONTAINING HIGH AND LOW PHOSPHORUS (43)

Alloy	4140		
Form	Bar		
Condition	Quenched and Tempered to Two Hardness Levels		
Exposure to 6000 psi H_2 at 75 F[b]	NTS, ksi[a]	HRC	F_{tu}, ksi
None	257	48	230
25 Days[c]	170	47	–
50 Days[c]	165	46	–
55 Days[c]	169	47	–
10 Days in Air After 55-Day Exposure	260	47	–
1 Day in Air After 25-Day Exposure	251	47	–
None	169	30	130
25 Days[c]	167	31	–
50 Days[c]	169	30	–
55 Days[c]	170	30	–

(a) Notched specimen.

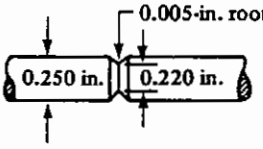

(b) Specimens under nominal tensile stress of 33,000 psi during exposures to hydrogen.

(c) Tested in air within 23 minutes after removal from hydrogen pressure chamber.

TABLE 1.0931. EFFECTS OF EXPOSURE TO HIGH-PRESSURE HYDROGEN ON NOTCHED TENSILE STRENGTH (8)

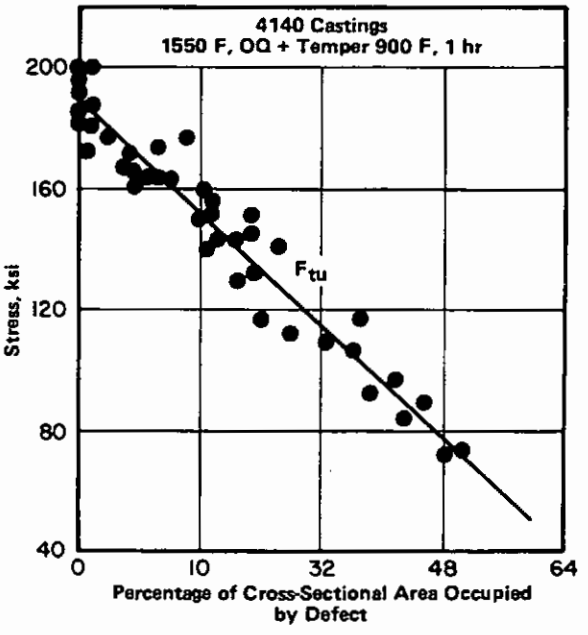

FIGURE 1.0951. EFFECT OF GAS HOLES AND SHRINKAGE DEFECTS ON TENSILE STRENGTH OF CASTINGS (3)

	Fe
0.4	C
1	Cr
0.2	Mo

4140

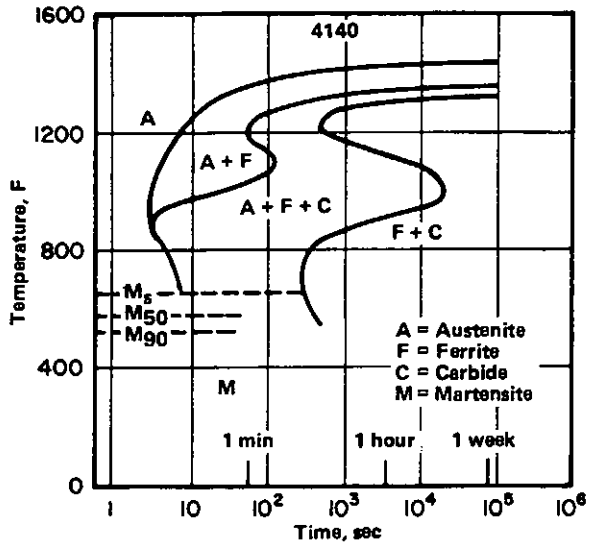

FIGURE 2.0121. TIME-TEMPERATURE-TRANSFORMATION DIAGRAM (12)

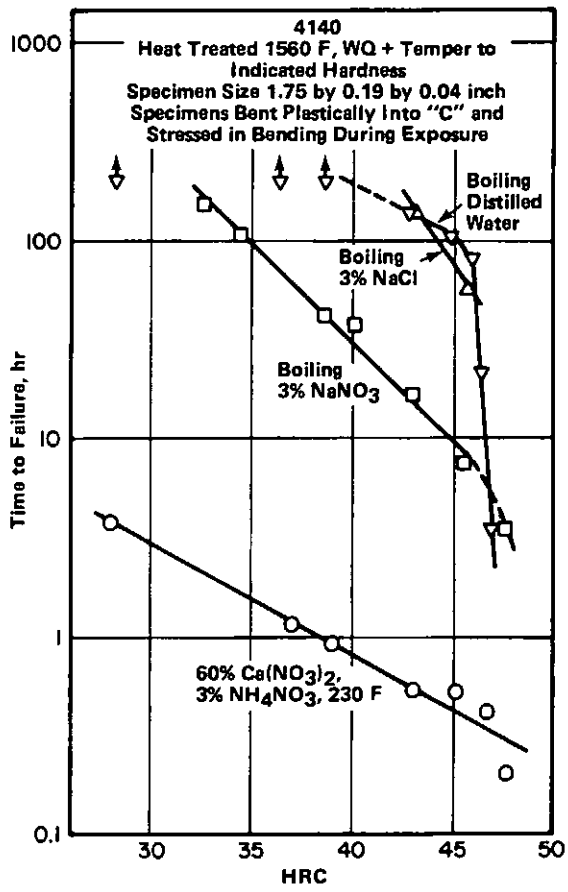

FIGURE 2.0312. EFFECT OF HEAT TREATED HARDNESS ON STRESS CORROSION CRACKING IN AQUEOUS SOLUTIONS (44, 45)

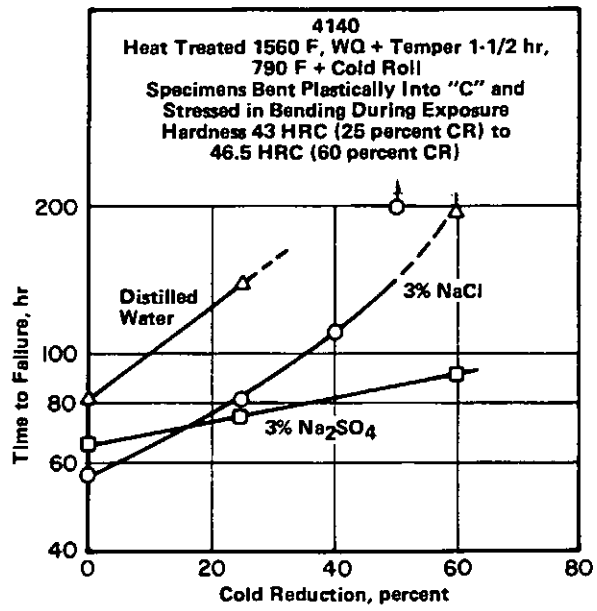

FIGURE 2.0314. EFFECT OF COLD ROLLING ON STRESS CORROSION CRACKING IN BOILING AQUEOUS SOLUTIONS (45)

Fe
0.4 Cr
1 Cr
0.2 Mo

4140

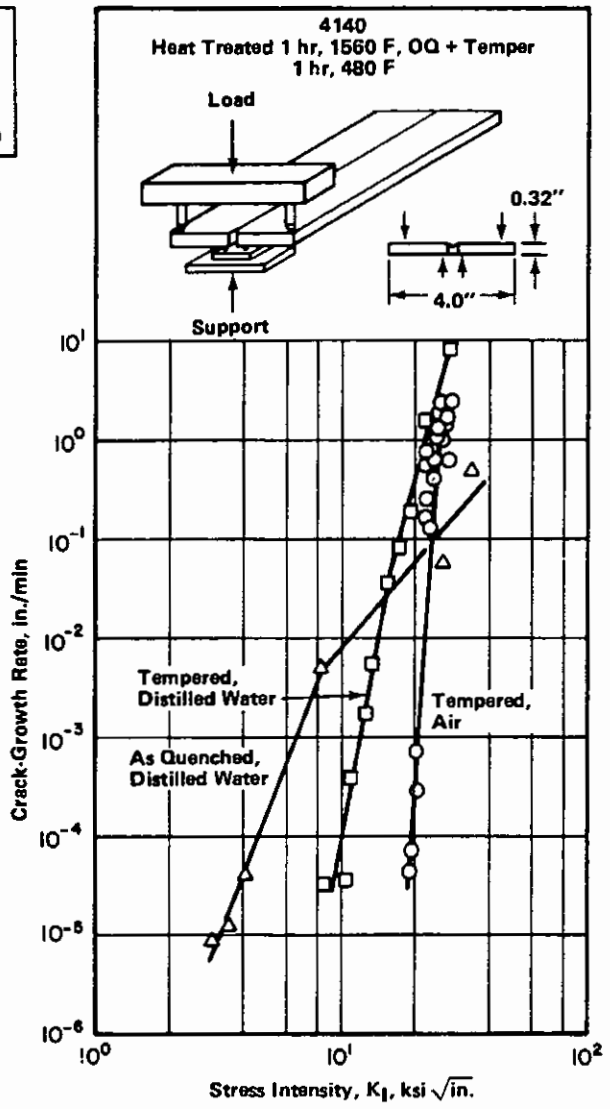

FIGURE 2.0317. STRESS CORROSION CRACK-GROWTH RATE AS A FUNCTION OF STRESS INTENSITY IN WATER AND IN AIR AT ROOM TEMPERATURE (60)

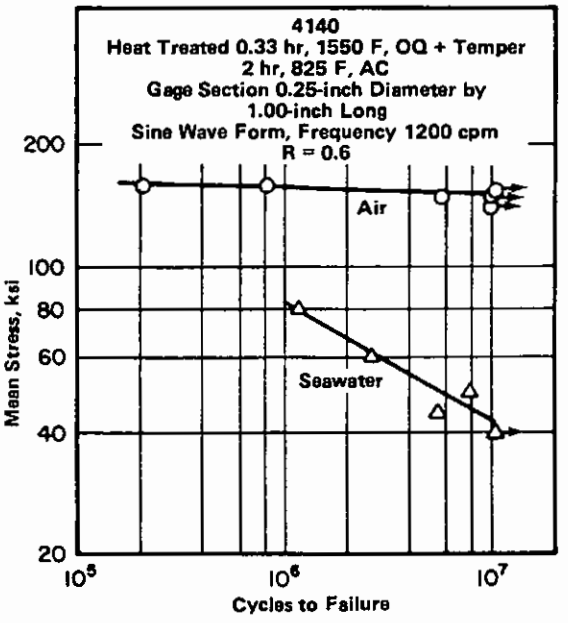

FIGURE 2.0319. CORROSION FATIGUE IN NATURAL SEAWATER AS COMPARED TO AIR AT ROOM TEMPERATURE (61)

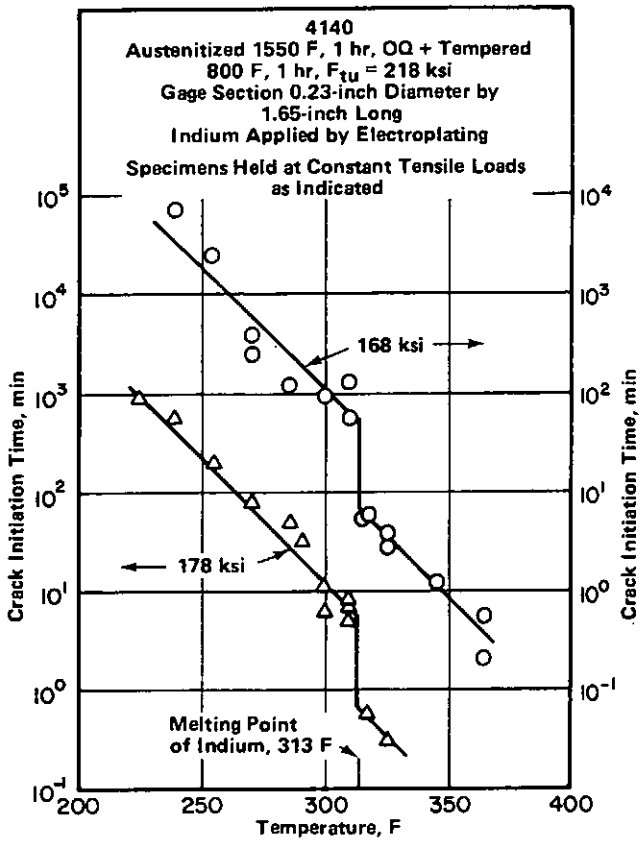

FIGURE 2.0332. DELAYED FRACTURE OF 4140 STEEL CAUSED BY METAL-INDUCED EMBRITTLEMENT WITH INDIUM (48)

FIGURE 2.0332. DELAYED FRACTURE OF 4140 STEEL CAUSED BY METAL-INDUCED EMBRITTLEMENT WITH INDIUM (48)

Alloy	4140										
AMS Specification	Product Form	Metallurgical Condition	Thickness, in.	F_{tu}, ksi Min	F_{tu}, ksi Max	F_{ty}, ksi, Min	Elongation, %, Min	RA, %, Min	Hardness[a] Min	Hardness[a] Max	Bend Angle, degrees[b]
5338C	Castings	Tempered	–	175	–	160	3	6	38 HRC	43 HRC	–
6378C	Bars	Hot Die-Drawn	–	150	–	130	5	20	(302 HBN)	(341 HBN)	–
6381C, 6390B	Tubing	Cold Finished	–	–	–	–	–	–	–	25 HRC	–
		Hot Finished	–	–	–	–	–	–	–	99 HRB	–
6382J	Bars, Forgings, and Rings	Cold Finished	≤0.50	–	125	–	–	–	–	–	–
		Cold Finished	>0.50	–	–	–	–	–	–	241 HBN	–
		Hot Finished	>0.50	–	–	–	–	–	–	229 HBN	–
6395B	Sheet, Strip, and Plate	–	"Sheet, Strip"	–	–	–	–	–	–	98 HRB	–
		–	"Plate"	–	–	–	–	–	–	25 HRC	–
		Tempered	≤0.875	180	–	–	–	–	(40 HRC)	–	–
		–	≤0.249	–	–	–	–	–	–	–	180
		–	0.249 – 0.749	–	–	–	–	–	–	–	90

Note: The original AMS documents should be consulted for complete specification details.

(a) Hardness specifications in parentheses need not be met if tensile specifications are met.
(b) Free bend around a diameter equal to the nominal thickness of the product.

TABLE 3.011. AMS SPECIFIED MECHANICAL PROPERTIES AT ROOM TEMPERATURE (17–22)

Fe
0.4 Cr
1 Cr
0.2 Mo

4140

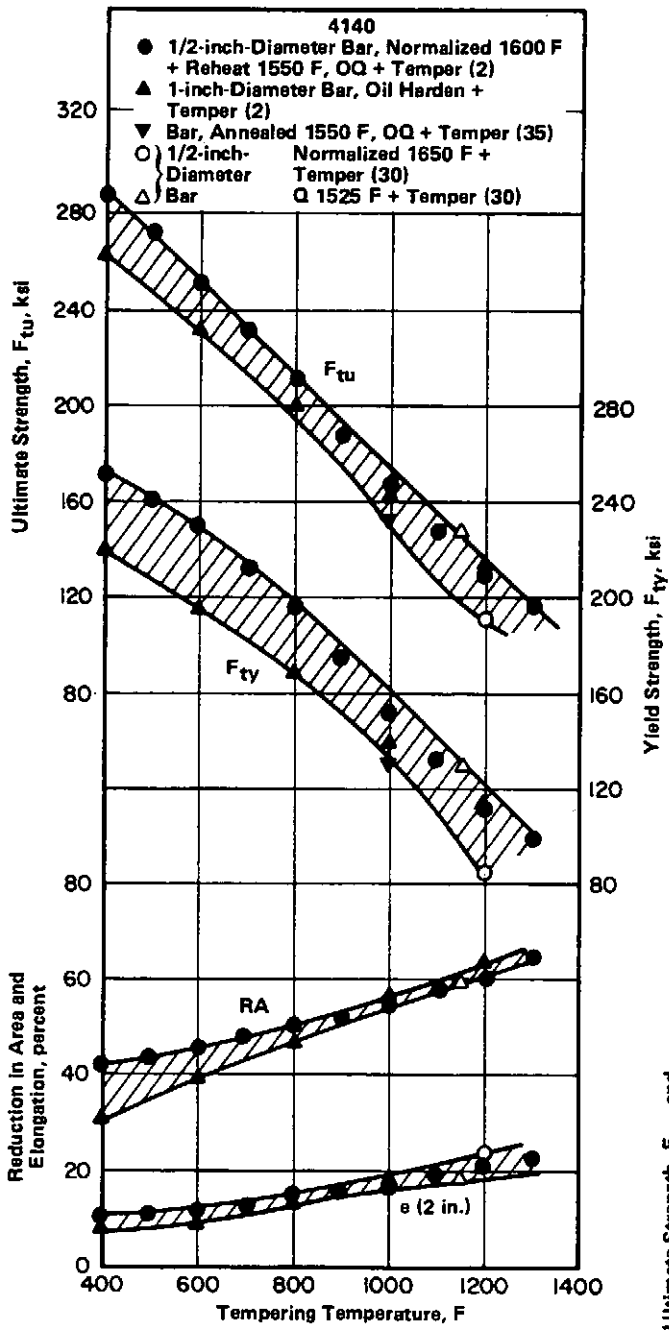

FIGURE 3.0211. EFFECT OF TEMPERING TEMPERATURE ON TENSILE PROPERTIES OF BAR (2, 30, 35)

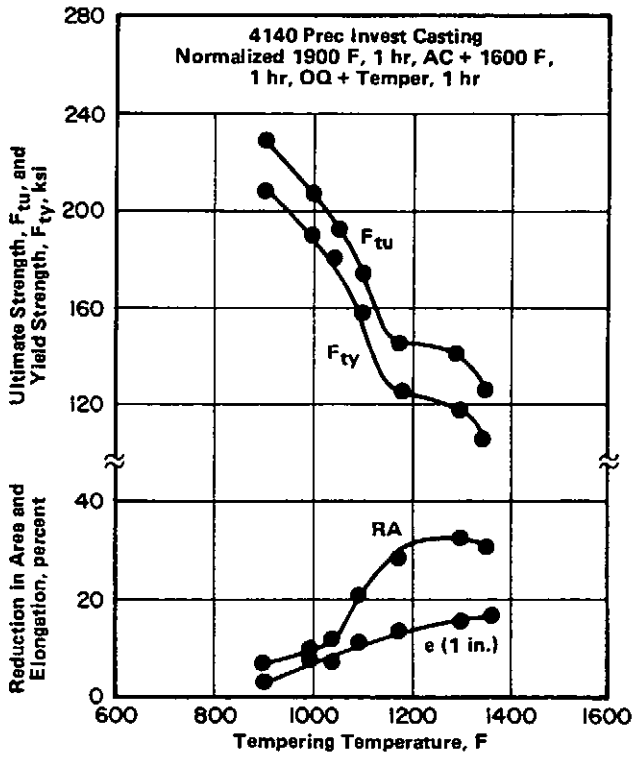

FIGURE 3.0212. EFFECT OF TEMPERING TEMPERATURE ON TENSILE PROPERTIES OF CASTINGS (36)

	Fe
0.4	C
1	Cr
0.2	Mo

4140

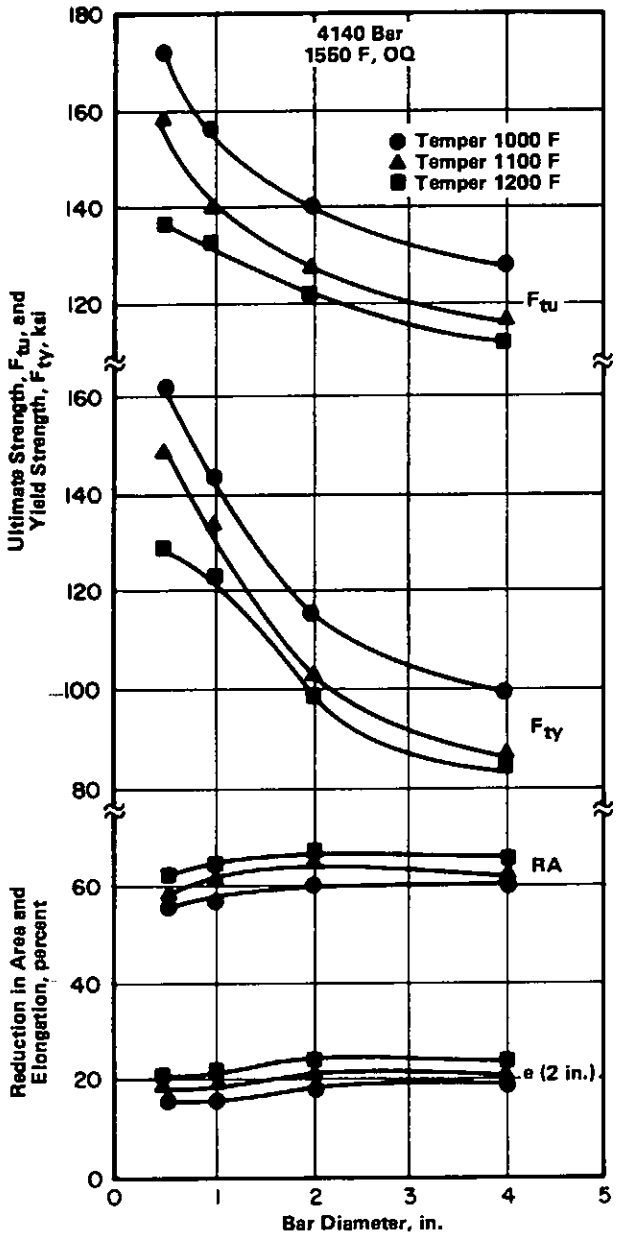

FIGURE 3.0213. EFFECT OF DIAMETER ON TENSILE PROPERTIES OF QUENCHED AND TEMPERED BAR (1)

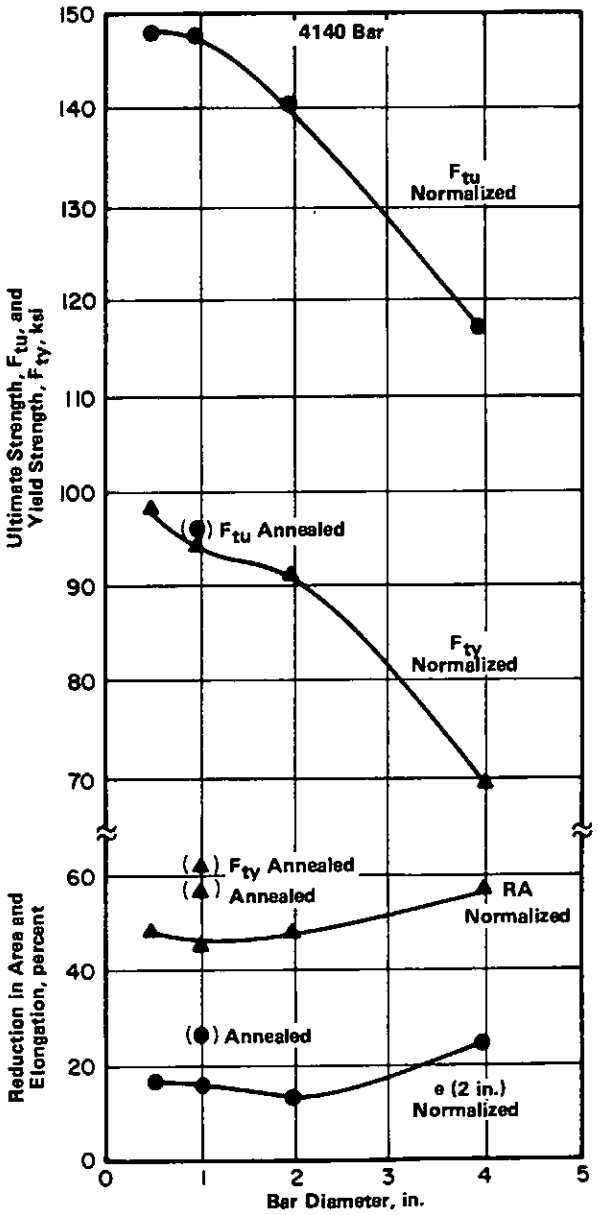

FIGURE 3.0214. TENSILE PROPERTIES OF NORMALIZED BARS FROM 1/2 TO 4 INCHES IN DIAMETER AND OF ANNEALED BAR 1.0 INCH IN DIAMETER (1)

Fe
0.4 Cr
1 Cr
0.2 Mo
4140

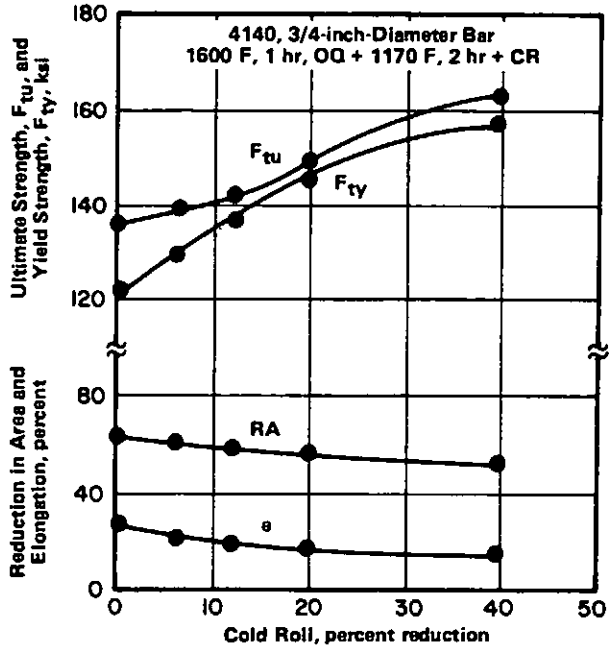

FIGURE 3.0215. EFFECT OF COLD ROLLING ON TENSILE PROPERTIES OF BAR (33)

Alloy	4140			
Form	Extrusions			
Condition	1550 F, OQ + Temper 600 F			
Specimen Orientation	F_{tu}, ksi	F_{ty}, ksi	e (2 in.), percent	RA, percent
Longitudinal	239	221	11.9	46.7
Transverse	230	210	4.7	17.0

TABLE 3.0216. TENSILE PROPERTIES OF EXTRUSIONS (10)

Alloy	4140							
Form	6-inch Diameter Bar							
Condition	OQ + Tempered to Two Hardness Levels							
		Nonleaded				Leaded			
HRC	Specimen Orientation	F_{tu}, ksi	F_{ty}, ksi	e (2 in.), percent	RA, percent	F_{tu}, ksi	F_{ty}, ksi	e (2 in.), percent	RA, percent
47	L	220	206	6.8	47.7	222	210	7.6	46.4
	T	166	126	3.5	3.3	169	126	2.8	6.5
55	L	269	228	7.9	45.2	272	246	5.8	36.6
	T	169	115	3.5	6.5	180	117	2.8	8.9

TABLE 3.0217. EFFECT OF SPECIMEN ORIENTATION ON TENSILE PROPERTIES OF 6-INCH-DIAMETER BAR HEAT TREATED TO TWO HARDNESS LEVELS (29)

Alloy	4140			
Form	Bar			
Condition	F_{tu}, ksi	F_{ty}, ksi	e (2 in.), percent	RA, percent
Hot Rolled	130 – 110	95 – 65	20 – 15	45 – 40
Annealed	100 – 90	70 – 65	27 – 25	55 – 50
Normalized	138 – 120	100 – 95	22 – 18	55 – 44

TABLE 3.0218. TENSILE PROPERTIES OF BAR IN UNHARDENED CONDITION (2)

Alloy	4140			
Form	Castings			
Condition	F_{tu}, ksi	F_{ty}, ksi	e (2 in.), percent	RA, percent
Annealed	90	60	25	45
Normalized	135	100	16	28
1600 F, WQ + Temper 1250 F, 5 hr	130	108	20	38

TABLE 3.0219. TENSILE PROPERTIES OF CASTINGS (2)

	Fe
0.4	C
1	Cr
0.2	Mo

4140

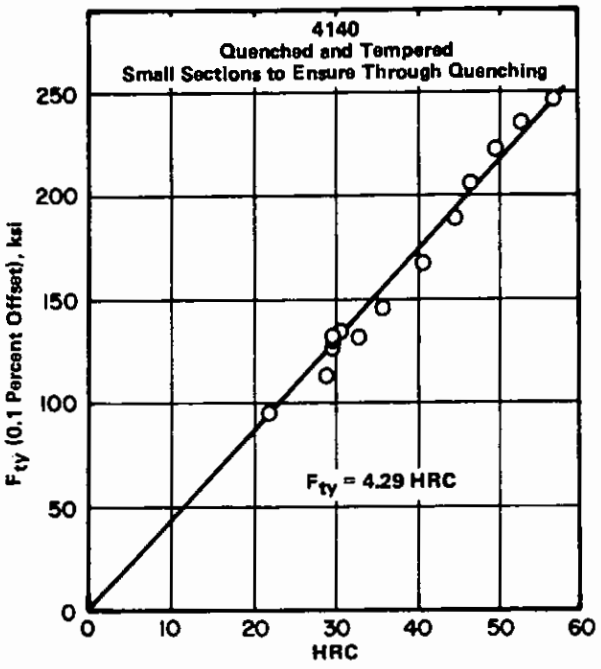

FIGURE 3.02110. RELATION BETWEEN YIELD STRENGTH AND HARDNESS FOR 4140 STEEL (62)

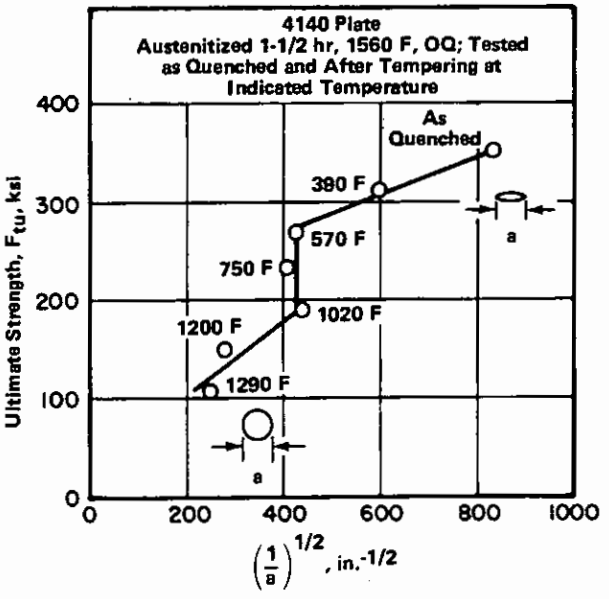

FIGURE 3.02112. VARIATION OF ULTIMATE TENSILE STRENGTH WITH CARBIDE SIZE AND SHAPE (50)

Fe
0.4 Cr
1 Cr
0.2 Mo
4140

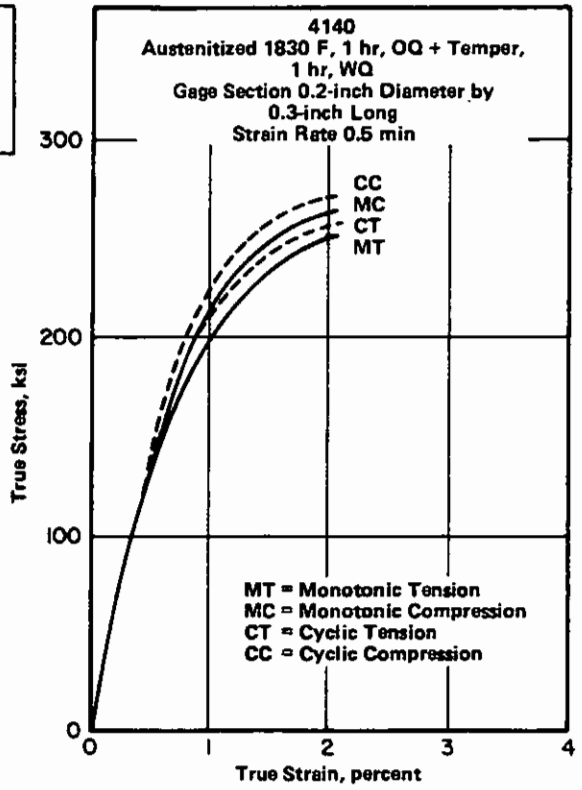

(a) Austenitized and Quenched

FIGURE 3.02114. MONOTONIC AND CYCLIC TRUE STRESS-TRUE STRAIN CURVES FOR 4140 STEEL (51)

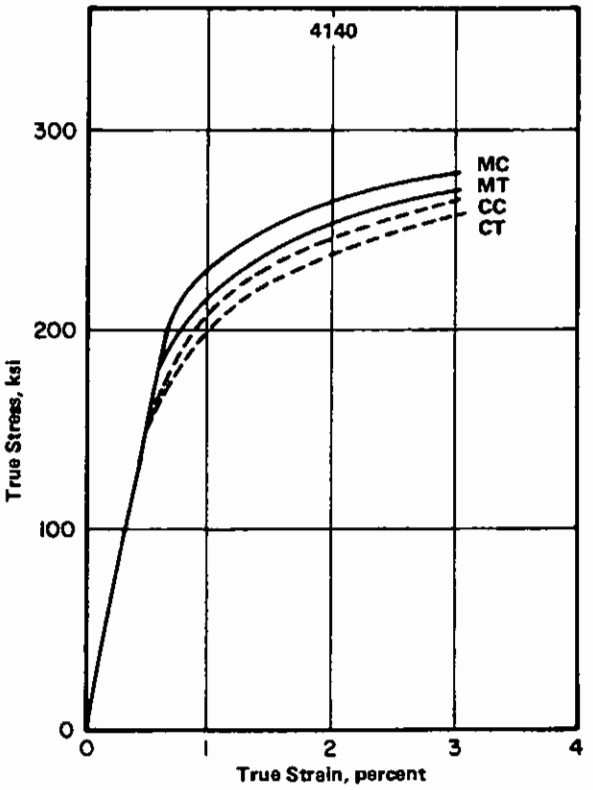

(b) Tempered at 390 F

FIGURE 3.02114. MONOTONIC AND CYCLIC TRUE STRESS-TRUE STRAIN CURVES FOR 4140 STEEL (51)

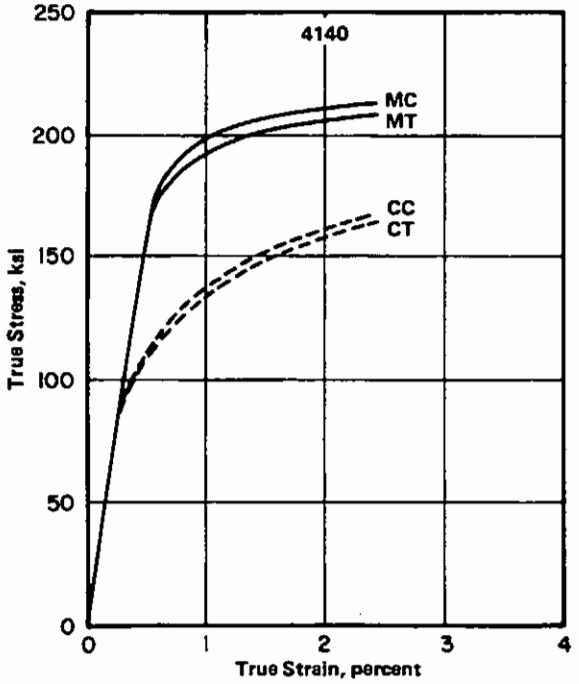

(c) Tempered at 750 F

FIGURE 3.02114. MONOTONIC AND CYCLIC TRUE STRESS-TRUE STRAIN CURVES FOR 4140 STEEL (51)

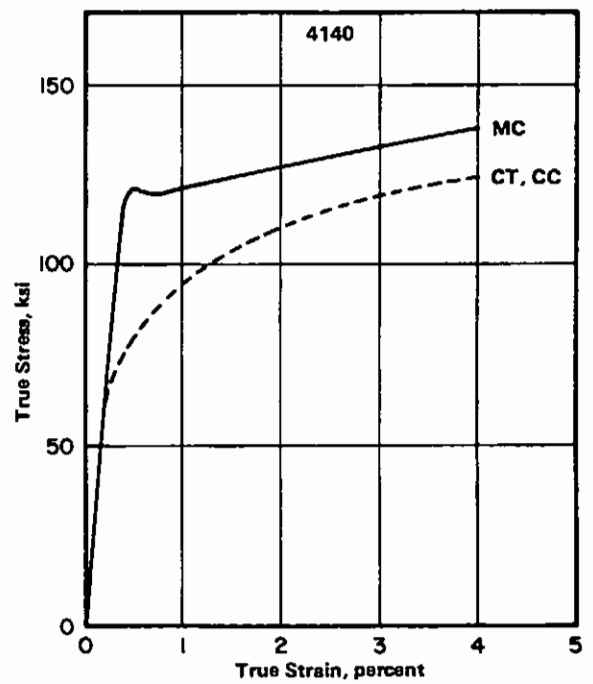

(d) Tempered at 1200 F

FIGURE 3.02114. MONOTONIC AND CYCLIC TRUE STRESS-TRUE STRAIN CURVES FOR 4140 STEEL (51)

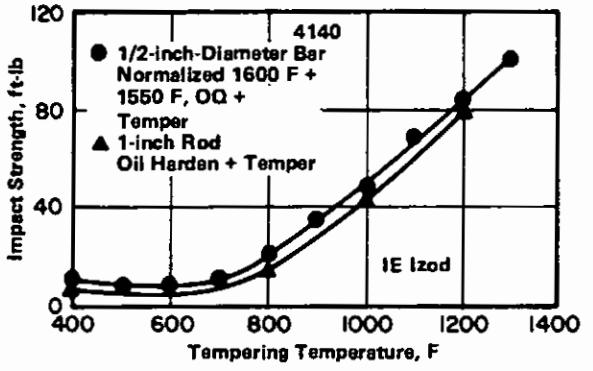

FIGURE 3.0231. EFFECT OF TEMPERING TEMPERATURE ON IMPACT PROPERTIES AT ROOM TEMPERATURE (2)

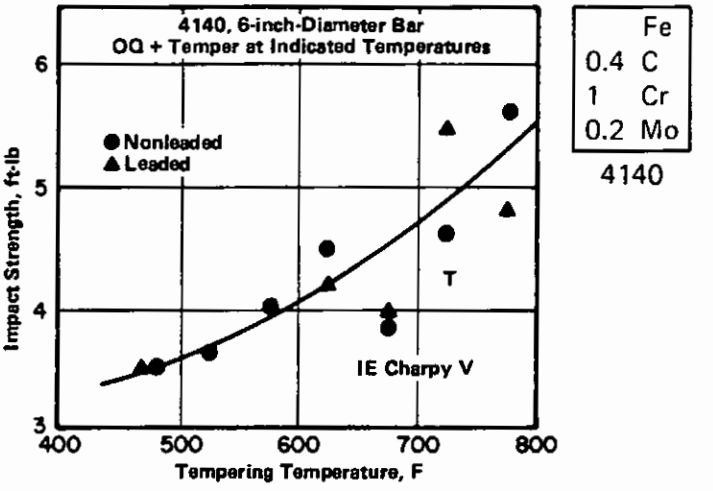

FIGURE 3.0232. TRANSVERSE IMPACT PROPERTIES OF LEADED AND NONLEADED 6-INCH-DIAMETER BAR AT ROOM TEMPERATURE (29)

Alloy	4140		
Form	Extruded Bar, 3/4 inch x 3-1/8 inch		
Condition	Specimen Orientation	Hardness	Impact, Charpy Keyhole, ft-lb
As Hot Extruded	L	89 HRB	25
	T	89 HRB	16
1550 F, OQ + Temper 600 F, 2 hr	L	49 HRC	14
	T	49 HRC	9
1550 F, OQ + Temper 900 F, 2 hr	L	40 HRC	23
	T	40 HRC	11

TABLE 3.0233. IMPACT PROPERTIES OF EXTRUDED BAR AT ROOM TEMPERATURE IN VARIOUS HEAT TREATED CONDITIONS (10)

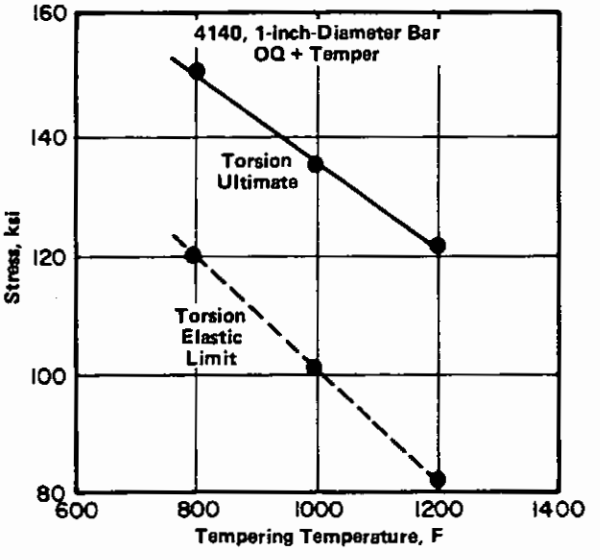

FIGURE 3.0251. EFFECT OF TEMPERING TEMPERATURE ON TORSIONAL PROPERTIES (2)

Fe
0.4 Cr
1 Cr
0.2 Mo

4140

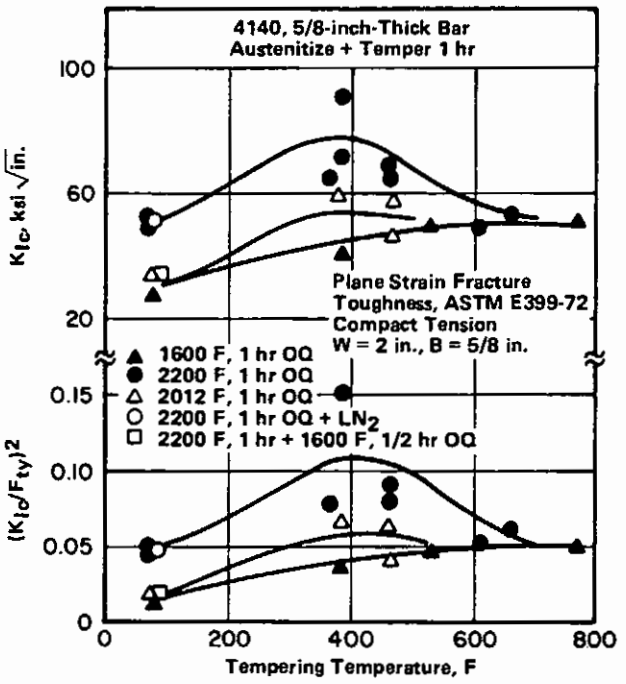

FIGURE 3.02721. EFFECT OF QUENCHING AND TEMPERING TEMPERATURE ON PLANE STRAIN FRACTURE TOUGHNESS (42)

Alloy	4140	
Condition	1550 F, 2 hr, Salt Quench to 325 F, AC + Double Temper 425 F, 2 hr	
Property	Type Test Uniaxial Tension	
F_{ty}, ksi	196	
F_{tu}, ksi	240	
e (2 in.), percent	5.5	
	Burst[a] With No Notch	
Biaxial Yield Strength (0.2 percent Offset), ksi	232	
Biaxial Ultimate Strength, ksi	265	
	Burst[a] With Fatigue-Cracked Through-Thickness Notch About 0.230-inch Long	
	Notch Environment	
	Air	Water
Hoop Stress at Fracture Start, ksi (σ i)	110	53
Hoop Stress at Burst, ksi (σ c)	115	73
	Burst With Machined Through-Thickness Notch (0.001-inch Root Rad), About 0.205-inch Long	
	Notch Environment	
	Air	Water
Hoop Stress at Fracture Start, ksi	69	51
Hoop Stress at Burst, ksi	124	67

(a) Burst tests by hydraulic pressurization of deep-drawn vessels 55-inches long, 11.45-inches ID, and 0.105 wall, open at one end. Notch located longitudinally 8 inches from open end.

TABLE 3.0281. BURST PROPERTIES OF SMALL PRESSURE VESSELS (11)

	Fe
0.4	C
1	Cr
0.2	Mo

4140

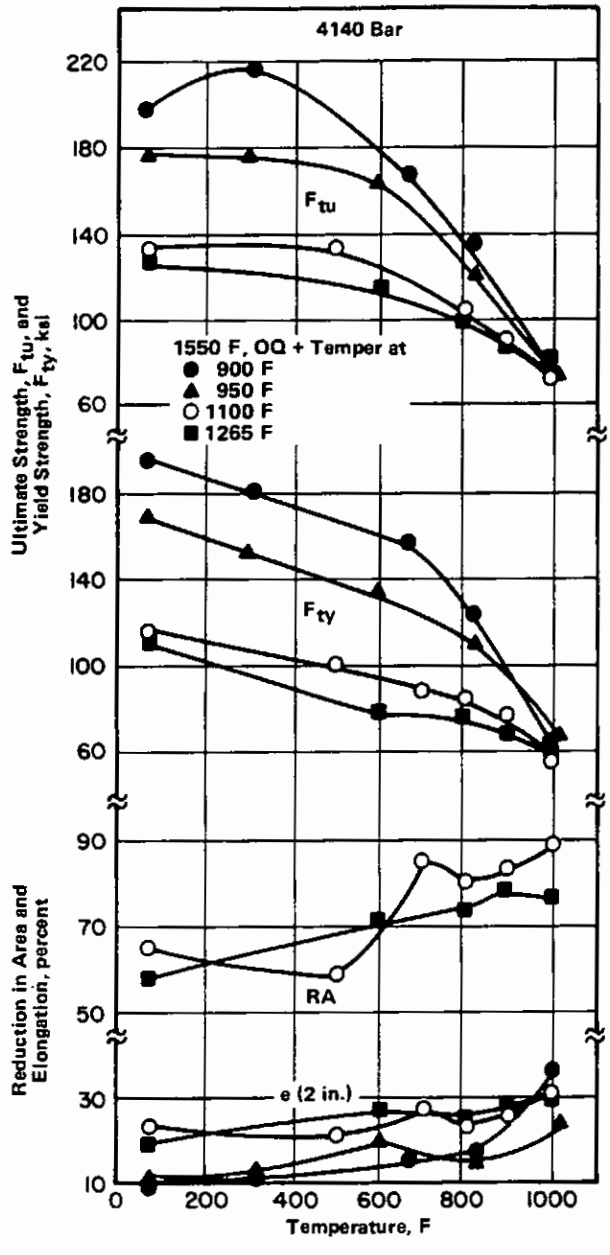

FIGURE 3.0311. EFFECT OF ELEVATED TEMPERATURES ON TENSILE PROPERTIES OF QUENCHED AND TEMPERED BAR (28)

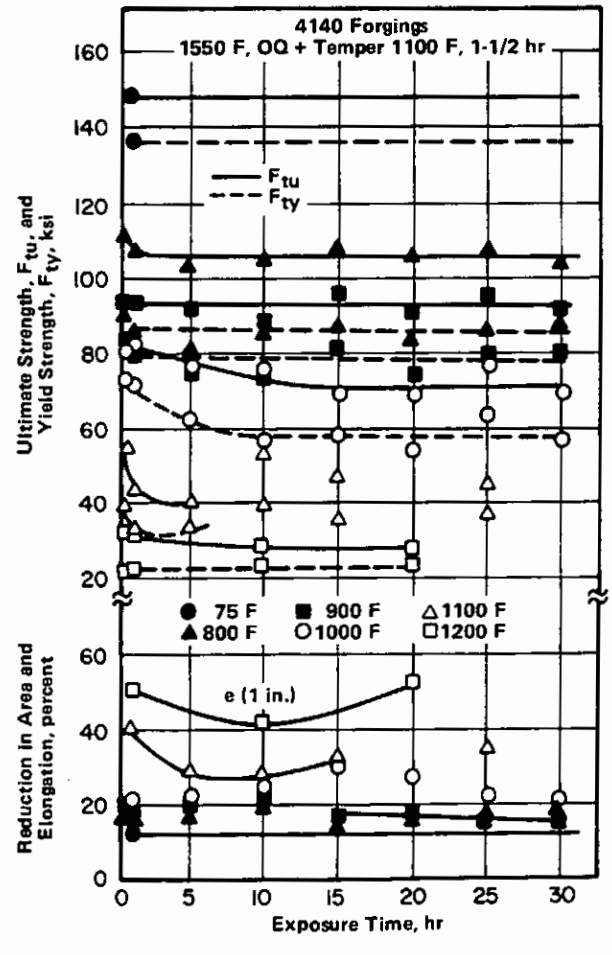

FIGURE 3.0312. EFFECT OF EXPOSURE TIME AND TEST TEMPERATURE ON ELEVATED TEMPERATURE TENSILE PROPERTIES (4)

Fe
0.4 Cr
1 Cr
0.2 Mo

4140

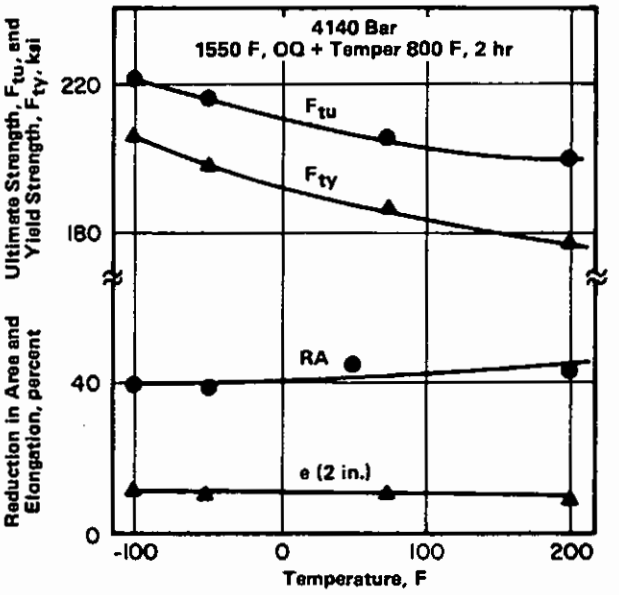

FIGURE 3.0313. EFFECTS OF TEMPERATURES FROM -100 F TO 200 F ON TENSILE PROPERTIES (39)

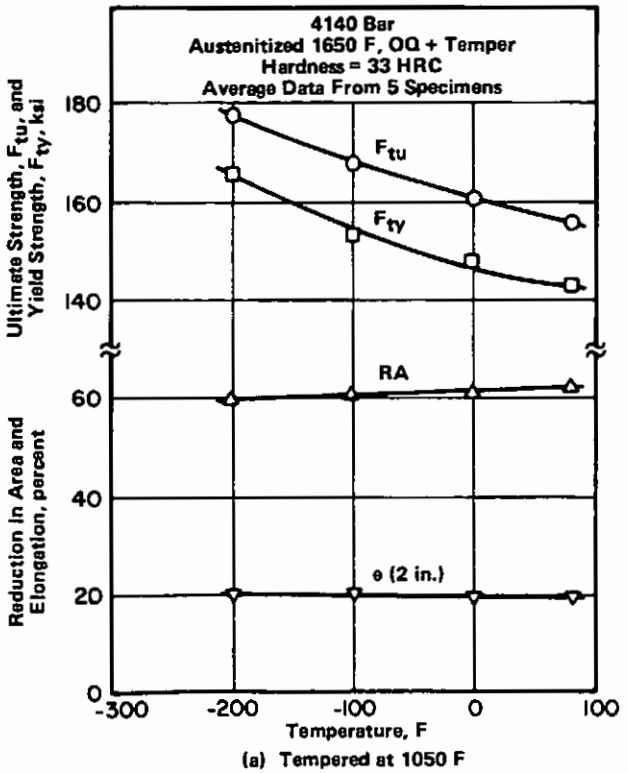

(a) Tempered at 1050 F

FIGURE 3.0314. EFFECTS OF TEMPERATURES FROM -200 F TO 80 F ON TENSILE PROPERTIES OF 4140 TEMPERED AT 1050 F AND AT 725 F (63)

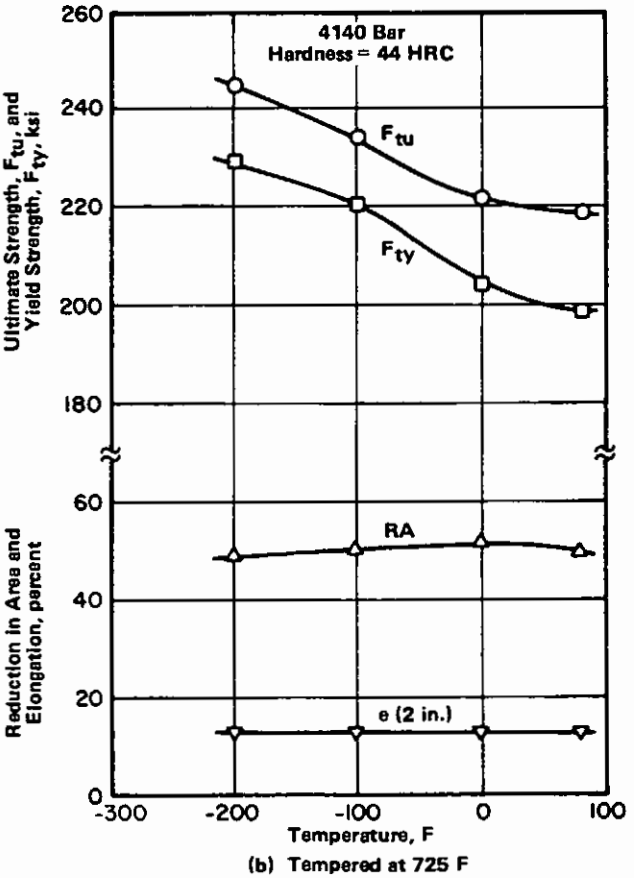

(b) Tempered at 725 F

FIGURE 3.0314. EFFECT OF TEMPERATURES FROM -200 F TO 80 F ON TENSILE PROPERTIES OF 4140 TEMPERED AT 1050 F AND AT 725 F (63)

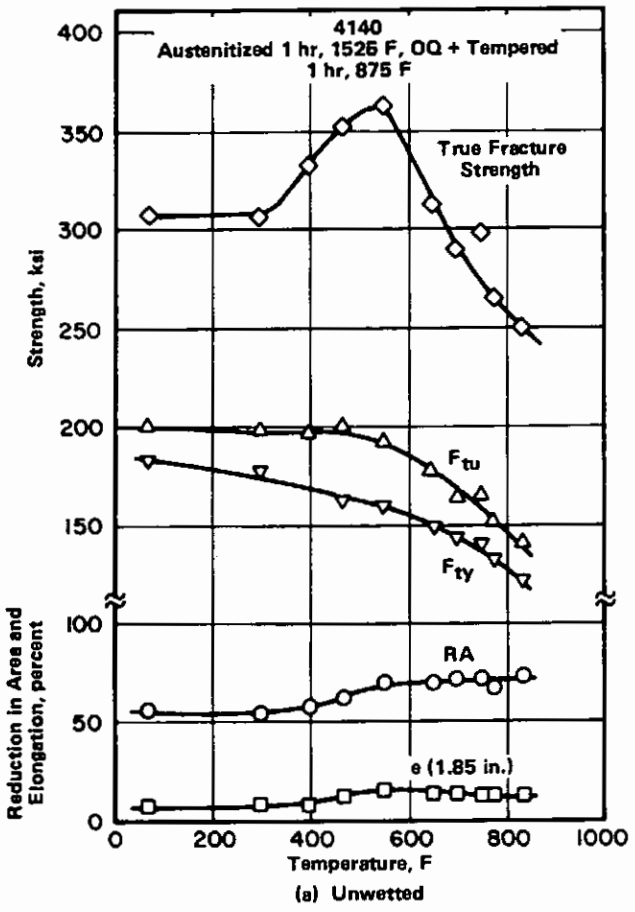

FIGURE 3.0316. EFFECTS OF SURFACE WETTING WITH LEAD ON TENSILE PROPERTIES (53)

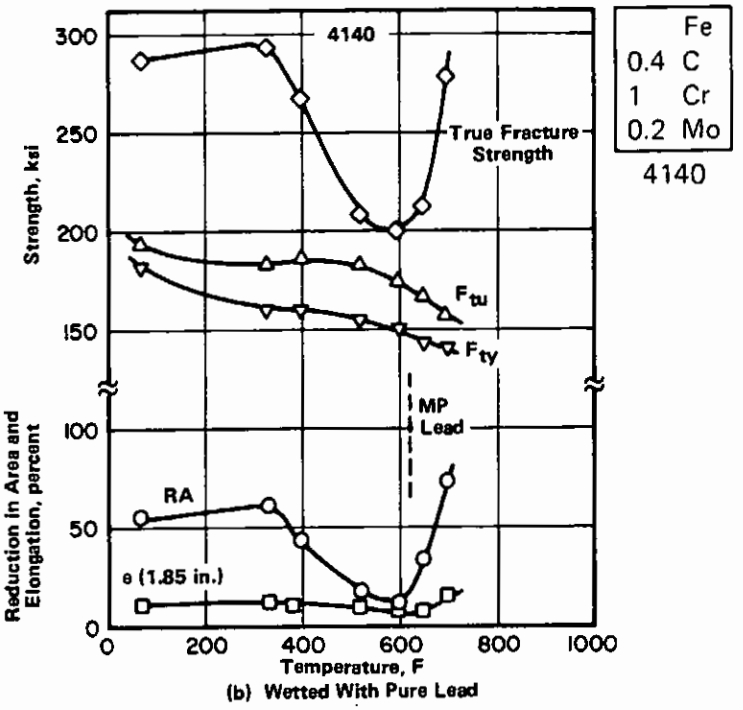

FIGURE 3.0316. EFFECTS OF SURFACE WETTING WITH LEAD ON TENSILE PROPERTIES (53)

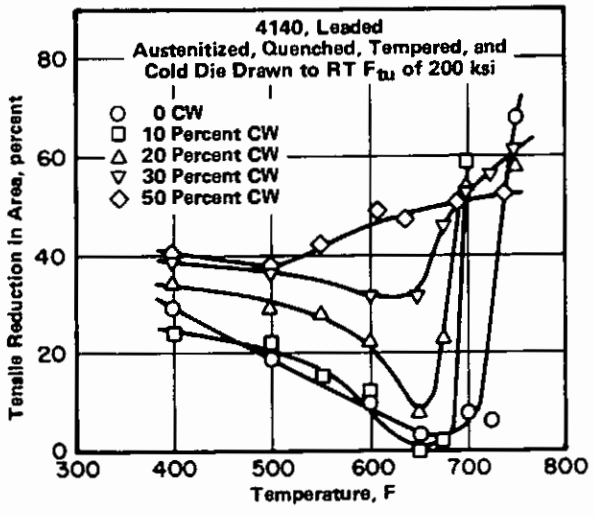

FIGURE 3.0318. ELIMINATION OF LEAD EMBRITTLEMENT BY PRIOR COLD DEFORMATION (54)

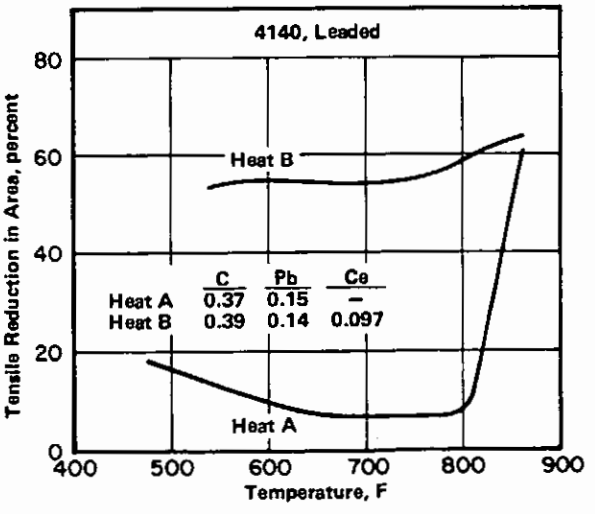

FIGURE 3.0319. ELIMINATION OF LEAD EMBRITTLEMENT BY THE ADDITION OF RARE EARTH ELEMENTS (54)

Fe
0.4 Cr
1 Cr
0.2 Mo

4140

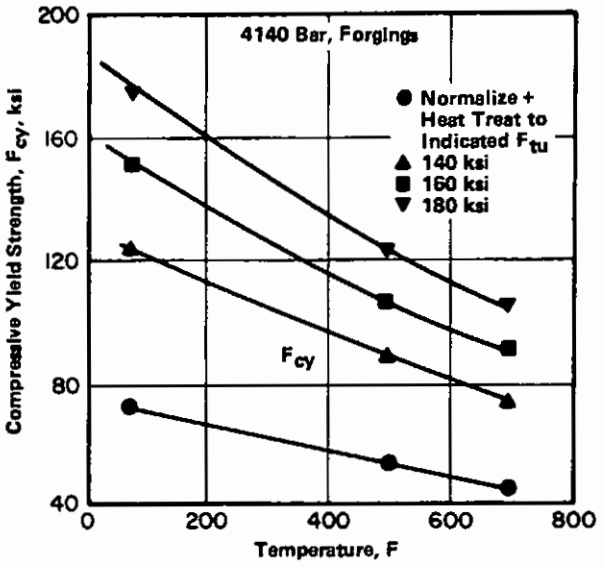

FIGURE 3.0321. EFFECT OF TEMPERATURE ON COMPRESSIVE YIELD STRENGTH OF BAR AND FORGINGS HEAT TREATED TO VARIOUS STRENGTH LEVELS (38)

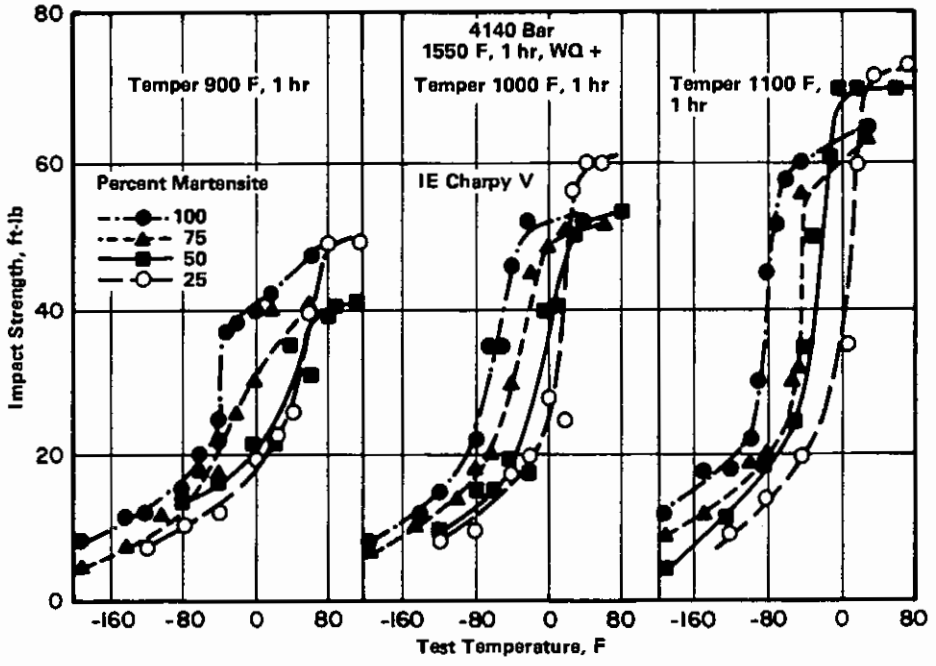

FIGURE 3.0331. EFFECTS OF TEST TEMPERATURE, TEMPERING TEMPERATURE, AND PERCENTAGE OF MARTENSITE IN MICROSTRUCTURE ON IMPACT PROPERTIES (6)

Note: Percent martensite controlled by use of specially designed end-quench specimens.

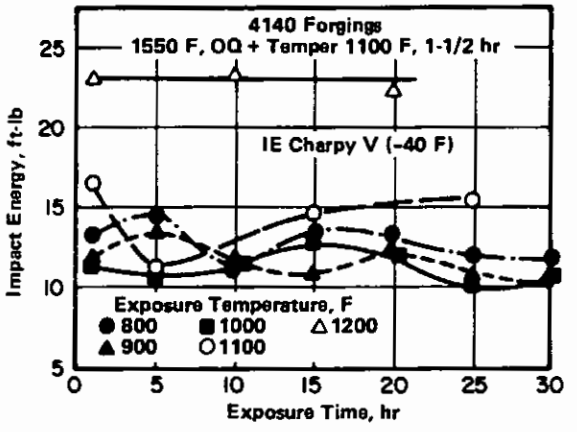

FIGURE 3.0332. EFFECTS OF EXPOSURES UP TO 30 HOURS AT VARIOUS ELEVATED TEMPERATURES ON IMPACT ENERGY AT -40 F (4)

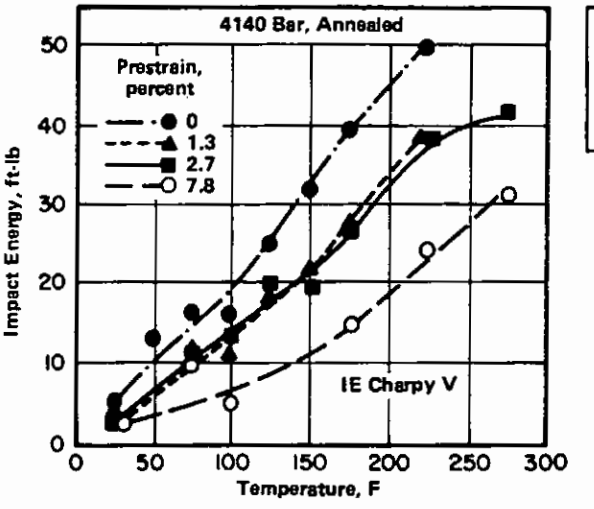

FIGURE 3.0333. EFFECTS OF TEMPERATURE AND PRE-STRAIN ON IMPACT ENERGY OF ANNEALED BAR (5)

Alloy	4140
Form	Castings
Condition	1600 F, WQ + Temper 1250 F, 5 hr
Temperature, F	Charpy V-Notch, ft-lb
70	22
-50	16

TABLE 3.0334. IMPACT PROPERTIES OF CASTINGS AT 70 AND -50 F (2)

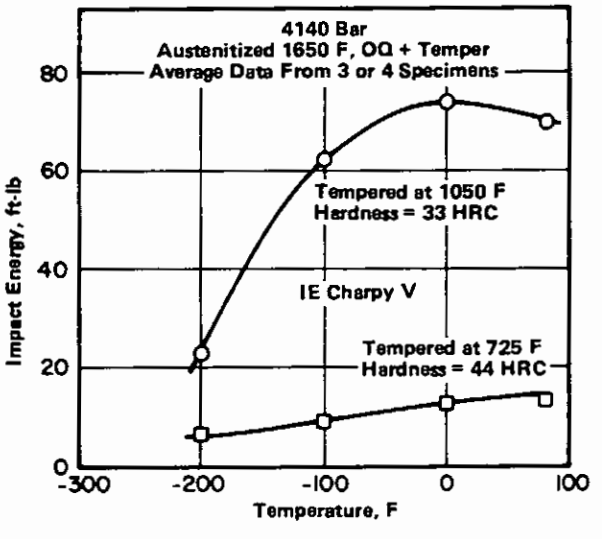

FIGURE 3.0335. EFFECTS OF TEMPERATURE FROM -200 F TO 80 F ON IMPACT ENERGY OF 4140 TEMPERED AT 1050 F AND AT 725 F (63)

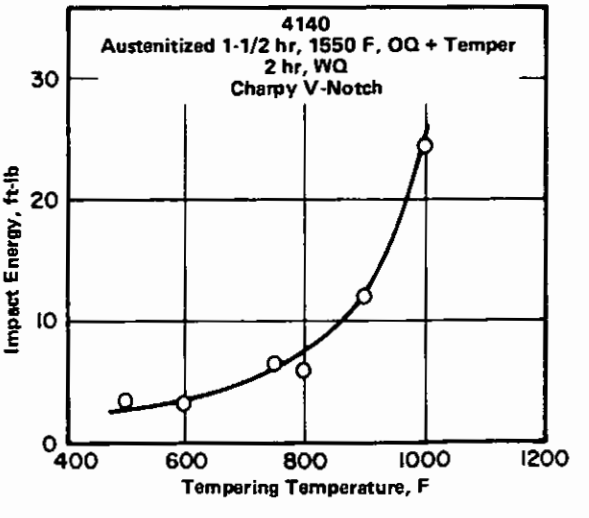

FIGURE 3.0336. EFFECT OF TEMPERING TEMPERATURE ON IMPACT ENERGY AT -40 F (64)

Fe
0.4 Cr
1 Cr
0.2 Mo

4140

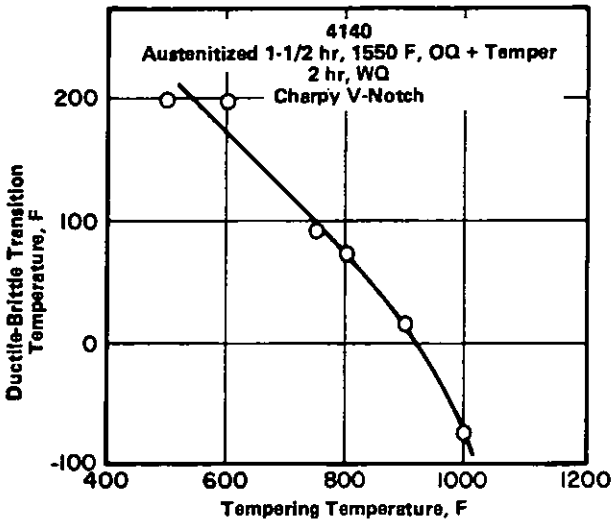

FIGURE 3.0337. EFFECT OF TEMPERING TEMPERATURE ON IMPACT DUCTILE-BRITTLE TRANSITION TEMPERATURE (64)

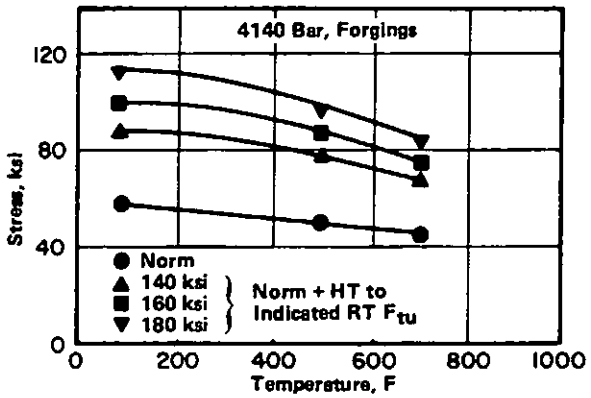

FIGURE 3.0351. EFFECT OF TEMPERATURE ON SHEAR STRENGTH OF BAR AND FORGINGS HEAT TREATED TO VARIOUS STRENGTH LEVELS (38)

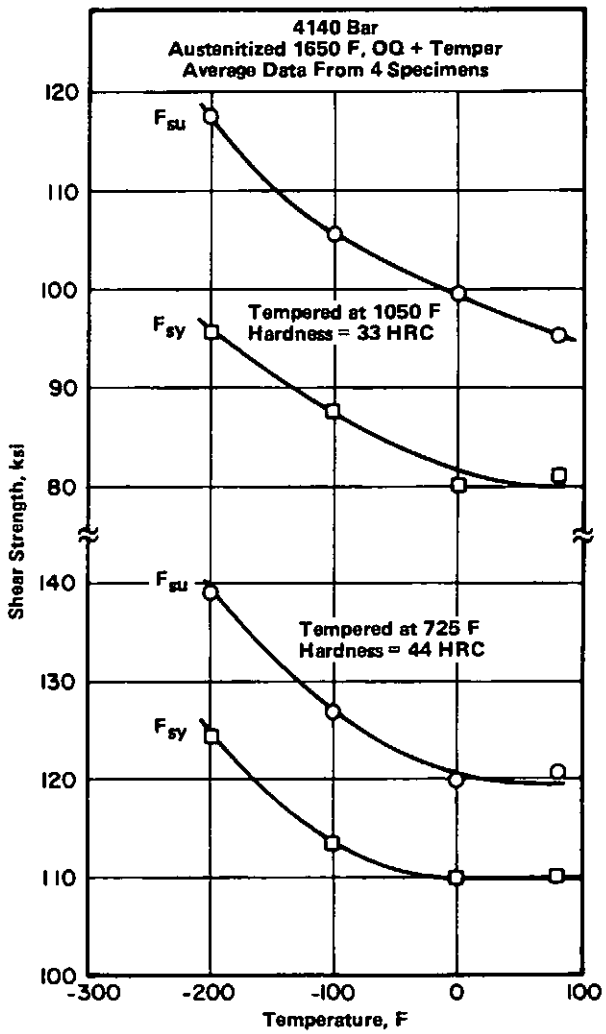

FIGURE 3.0352. EFFECTS OF TEMPERATURE FROM -200 F TO 80 F ON SHEAR STRENGTH OF 4140 TEMPERED AT 1050 F AND AT 725 F (63)

Fe
0.4 C
1 Cr
0.2 Mo

4140

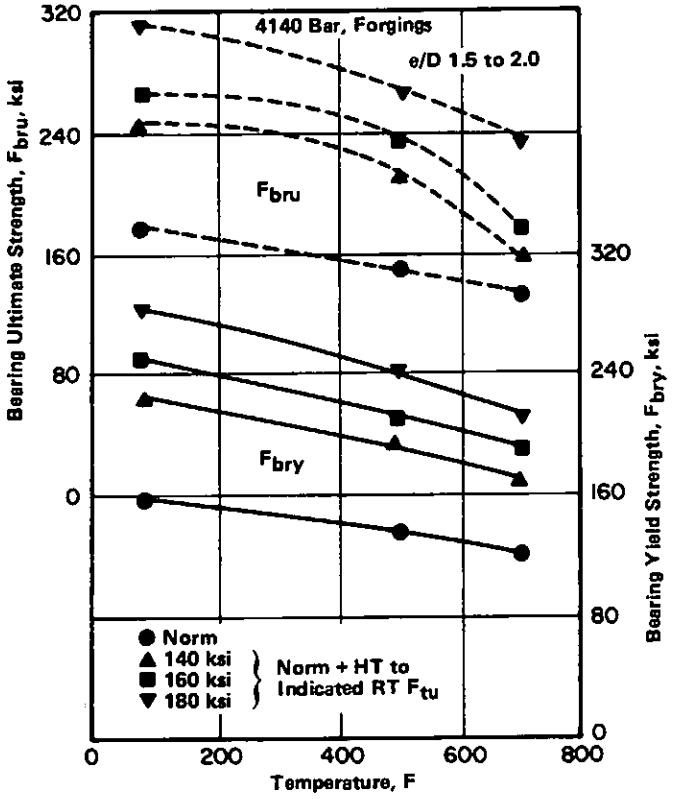

FIGURE 3.0361. EFFECT OF TEMPERATURE ON BEARING STRENGTH OF BAR AND FORGINGS HEAT TREATED TO VARIOUS STRENGTH LEVELS (38)

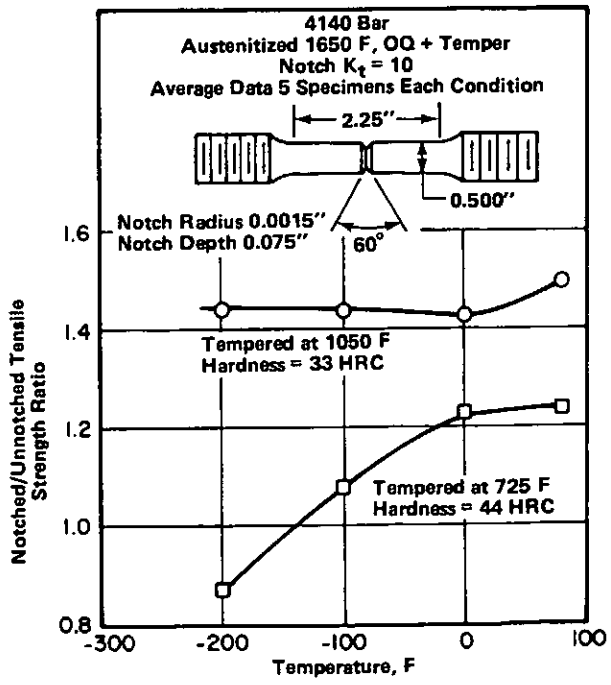

FIGURE 3.03711. EFFECTS OF TEMPERATURE FROM -200 F TO 80 F ON NOTCHED/UNNOTCHED TENSILE STRENGTH RATIO OF 4140 TEMPERED AT 1050 F AND AT 725 F (63)

Fe
0.4 Cr
1 Cr
0.2 Mo

4140

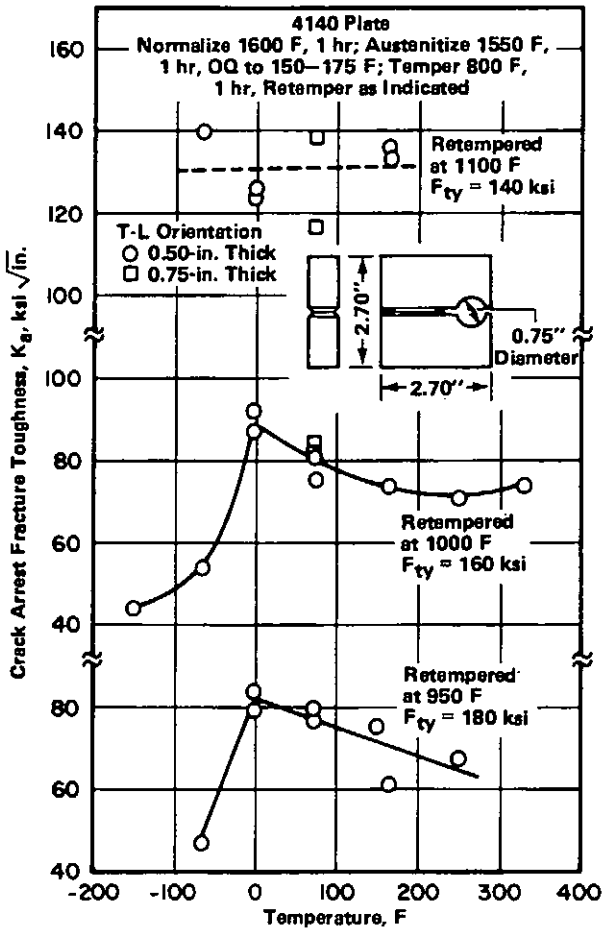

FIGURE 3.03722. CRACK ARREST FRACTURE TOUGHNESS OF 4140 STEEL AS A FUNCTION OF TEST TEMPERATURE (65)

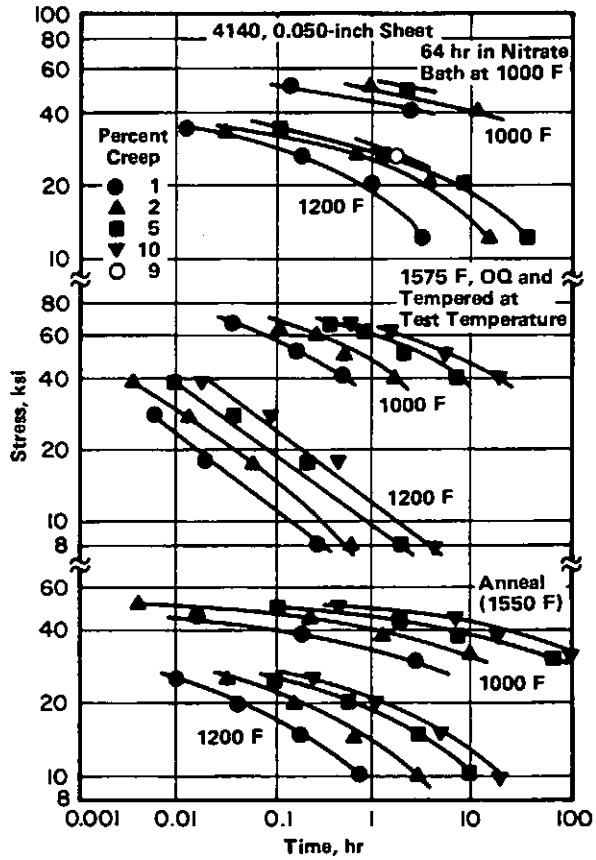

FIGURE 3.041. CREEP PROPERTIES AT 1000 F AND 1200 F OF SHEET IN VARIOUS HEAT TREATED CONDITIONS (40)

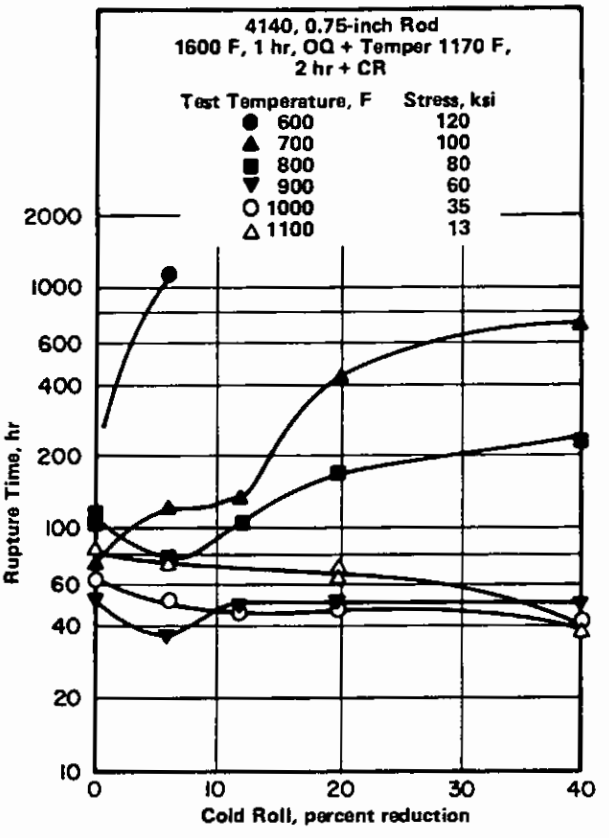

FIGURE 3.042. EFFECT OF COLD ROLLING ON CREEP-RUPTURE TIME OF QUENCHED AND TEMPERED ROD AT VARIOUS COMBINATIONS OF TEMPERATURE AND STRESS (33)

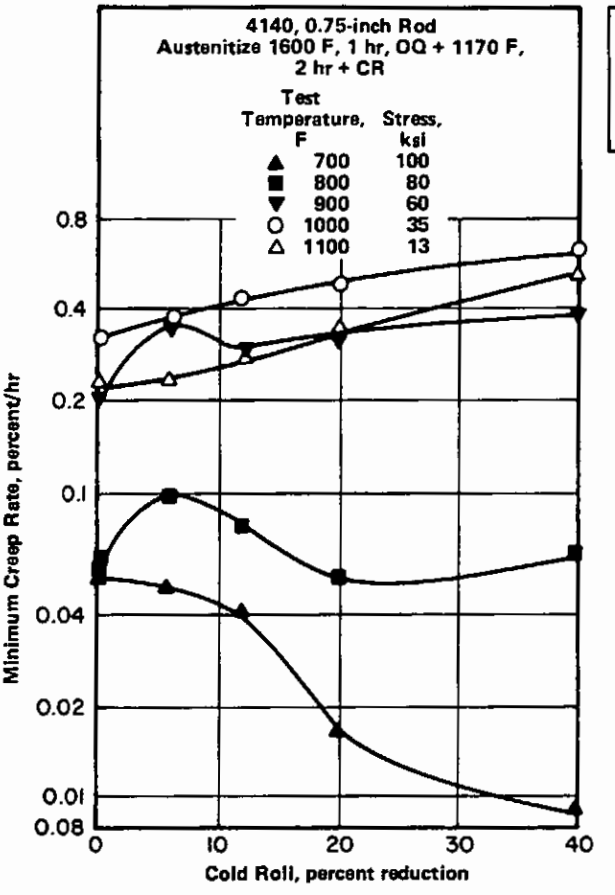

FIGURE 3.043. EFFECT OF COLD ROLLING ON MINIMUM CREEP RATE OF QUENCHED AND TEMPERED ROD AT VARIOUS COMBINATIONS OF TEMPERATURE AND STRESS (33)

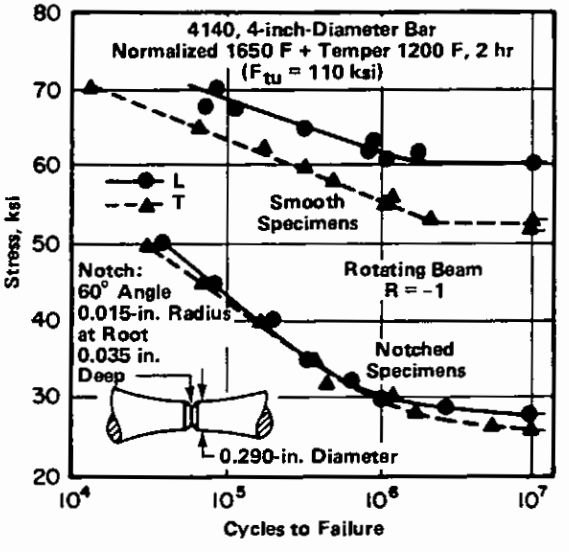

FIGURE 3.051. LONGITUDINAL AND TRANSVERSE FATIGUE PROPERTIES OF SMOOTH AND NOTCHED SPECIMENS (30)

Fe
0.4 Cr
1 Cr
0.2 Mo
4140

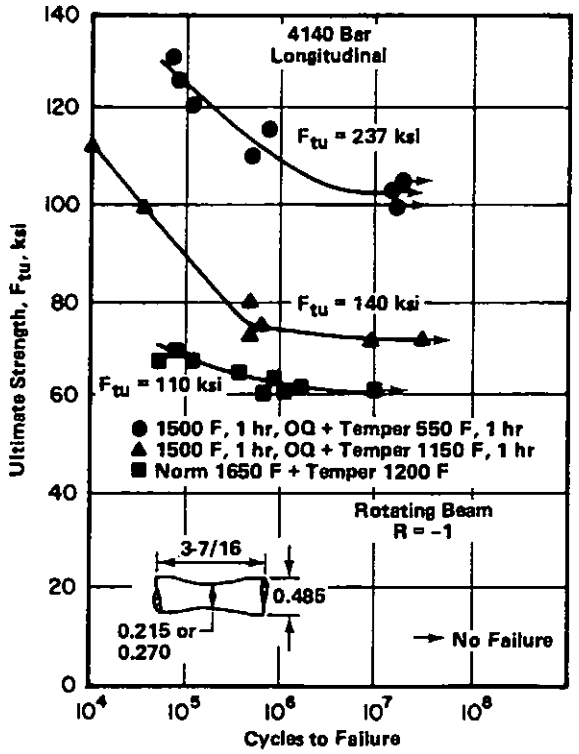

FIGURE 3.052. FATIGUE PROPERTIES OF SMOOTH BARS HEAT TREATED TO VARIOUS STRENGTH LEVELS (30, 31)

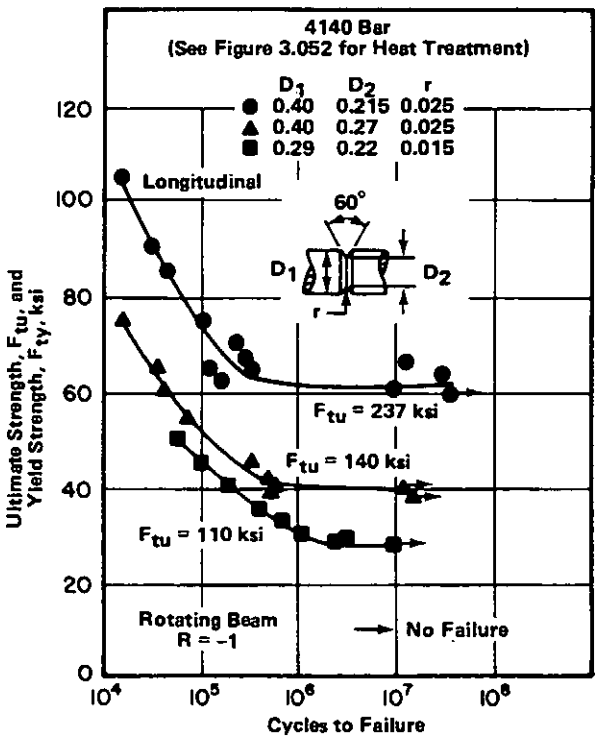

FIGURE 3.053. FATIGUE PROPERTIES OF NOTCHED BARS HEAT TREATED TO VARIOUS STRENGTH LEVELS (30, 31)

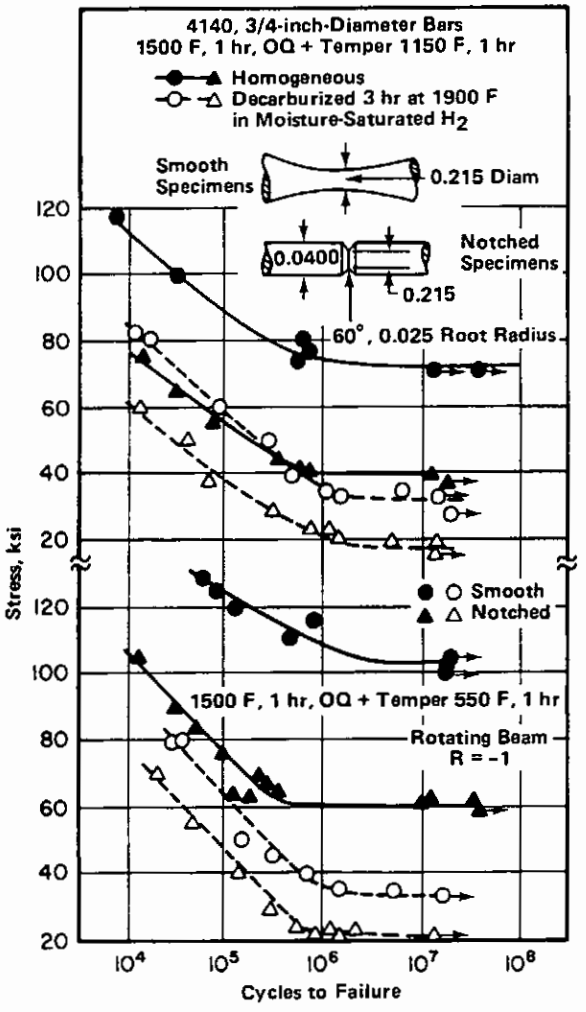

FIGURE 3.054. EFFECTS OF DECARBURIZATION ON FATIGUE PROPERTIES OF SMOOTH AND NOTCHED SPECIMENS (31)

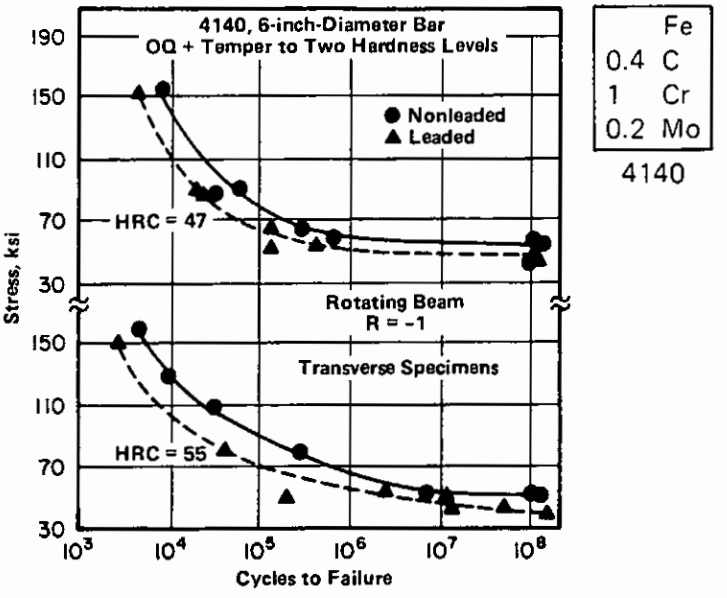

FIGURE 3.055. FATIGUE PROPERTIES OF LEADED AND NONLEADED BAR AT TWO HARDNESS LEVELS (29)

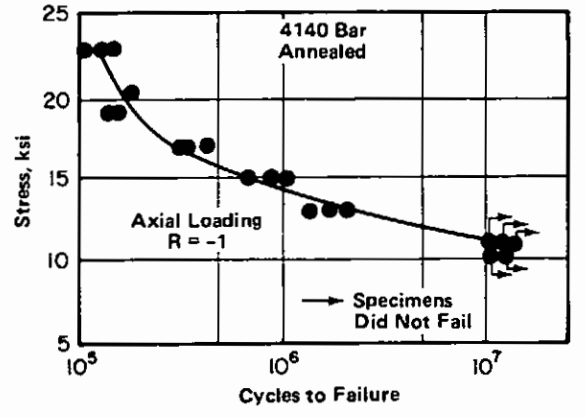

FIGURE 3.056. FATIGUE PROPERTIES OF ANNEALED BAR (5)

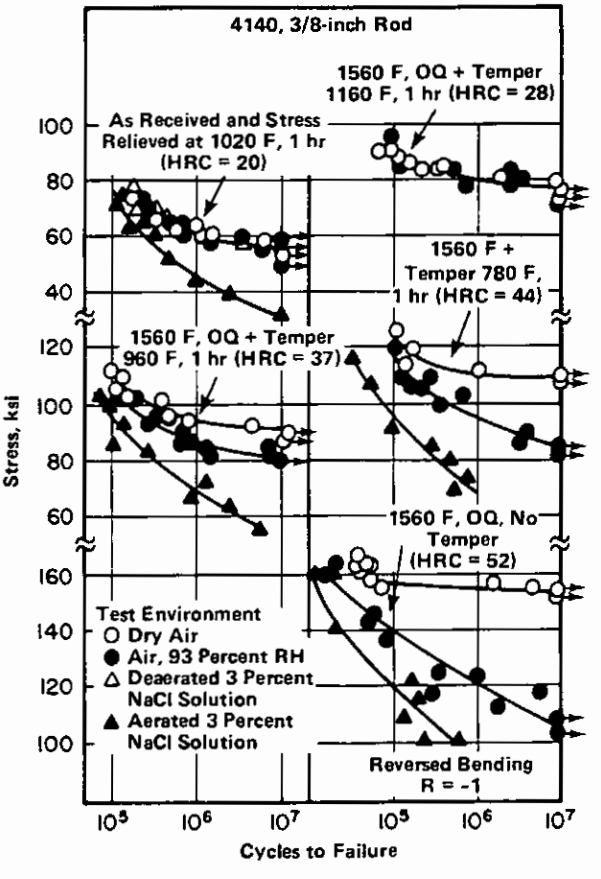

FIGURE 3.057. EFFECTS OF VARIOUS ENVIRONMENTS ON FATIGUE PROPERTIES IN DIFFERENT HEAT TREATED CONDITIONS (25)

Fe
0.4 Cr
1 Cr
0.2 Mo
4140

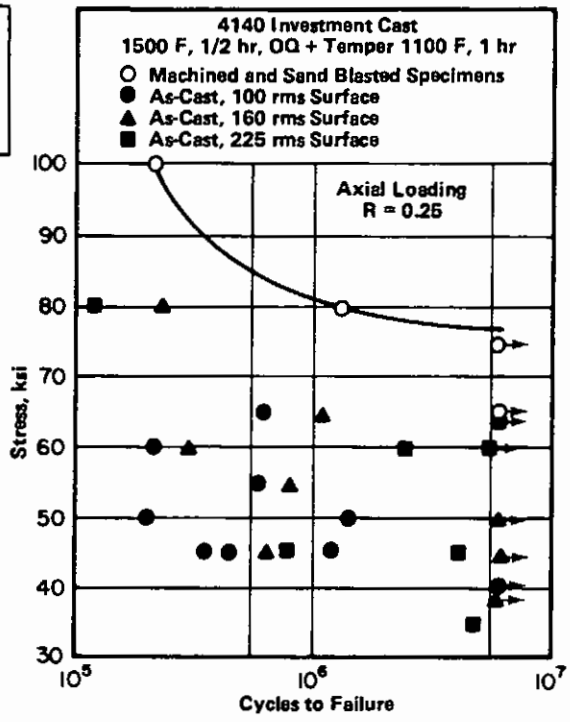

FIGURE 3.058. FATIGUE DATA FOR INVESTMENT CASTINGS SHOWING IMPROVEMENT IN FATIGUE LIFE AND CONSISTENCY OF RESULTS PRODUCED BY MACHINING AND SAND BLASTING (7)

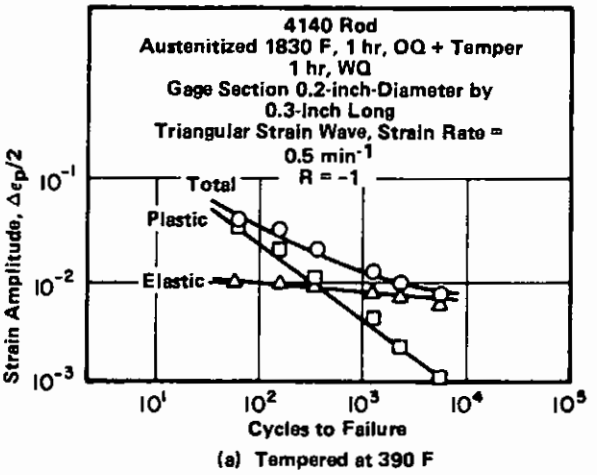

(a) Tempered at 390 F

FIGURE 3.059. ROOM TEMPERATURE FATIGUE BEHAVIOR OF QUENCHED AND TEMPERED 4140 (51)

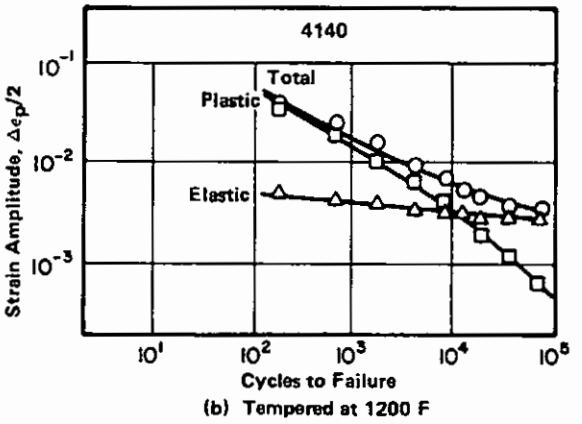

(b) Tempered at 1200 F

FIGURE 3.059. ROOM TEMPERATURE FATIGUE BEHAVIOR OF QUENCHED AND TEMPERED 4140 (51)

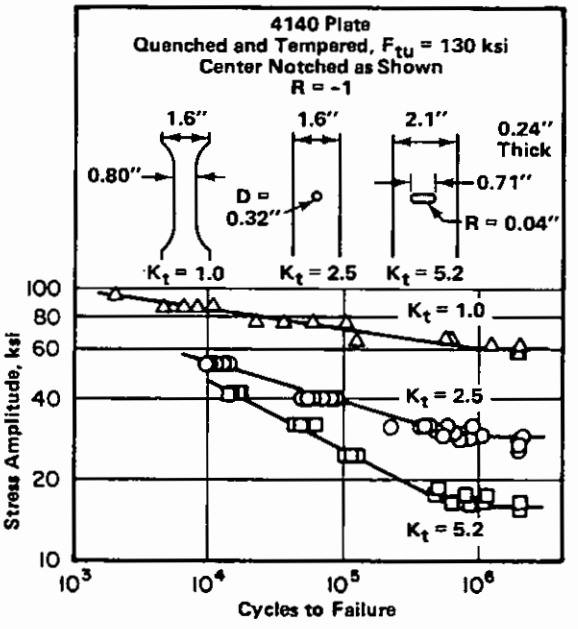

FIGURE 3.0510. EFFECTS OF NOTCHES ON CYCLIC FATIGUE LIFE AT ROOM TEMPERATURE (66)

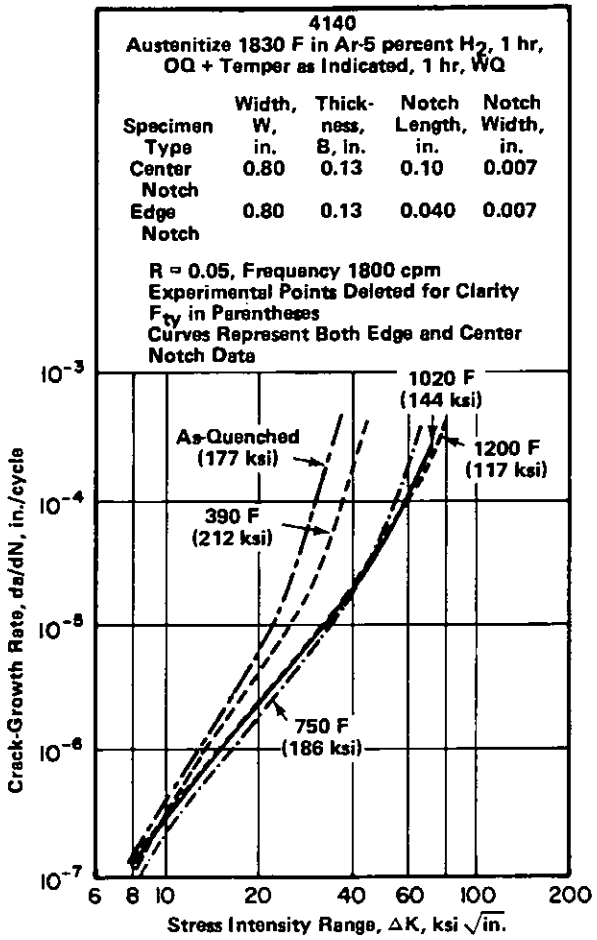

FIGURE 3.0512. ROOM TEMPERATURE FATIGUE CRACK GROWTH BEHAVIOR OF 4140 STEEL AUSTENITIZED AT 1830 F AND TEMPERED AT 390 F TO 1200 F (67)

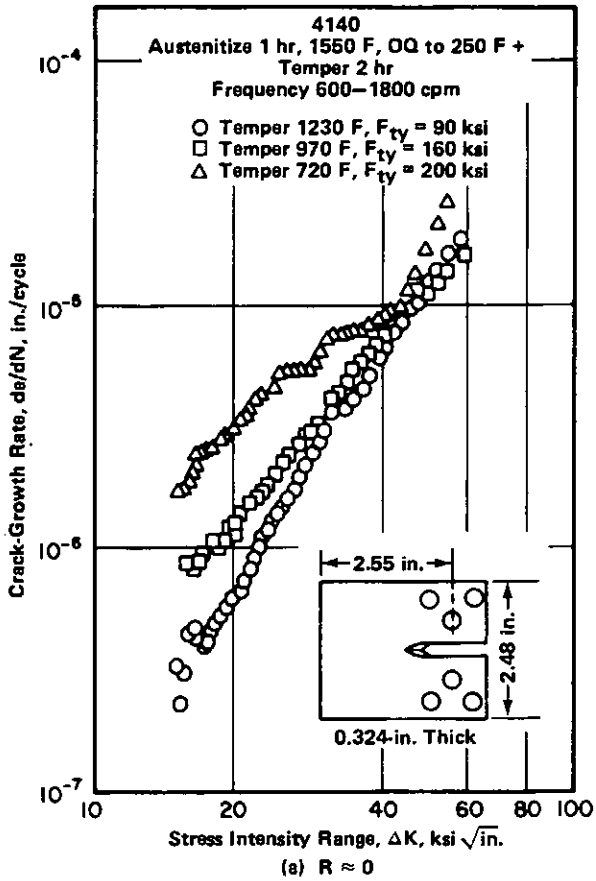

(a) R ≈ 0

Fe
0.4 C
1 Cr
0.2 Mo
4140

FIGURE 3.0513. ROOM TEMPERATURE FATIGUE CRACK-GROWTH BEHAVIOR OF 4140 STEEL AUSTENITIZED AT 1550 F AND TEMPERED AT 720 F TO 1230 F (68)

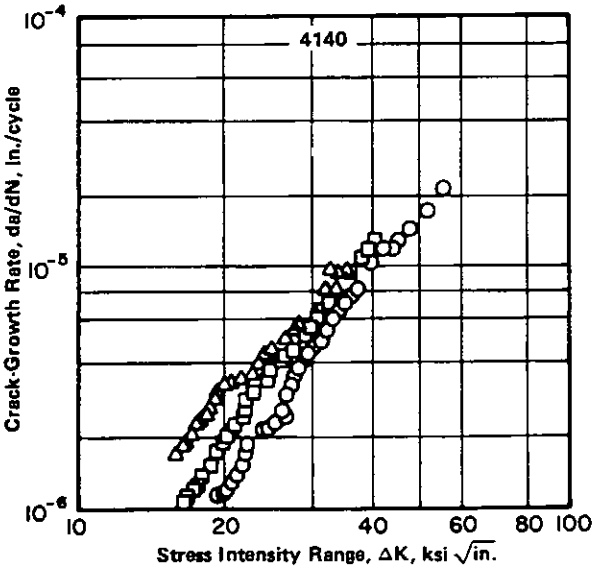

(b) R = -1

FIGURE 3.0513. ROOM TEMPERATURE FATIGUE CRACK-GROWTH RATE OF 4140 STEEL AUSTENITIZED AT 1550 F AND TEMPERED AT 720 F TO 1230 F (68)

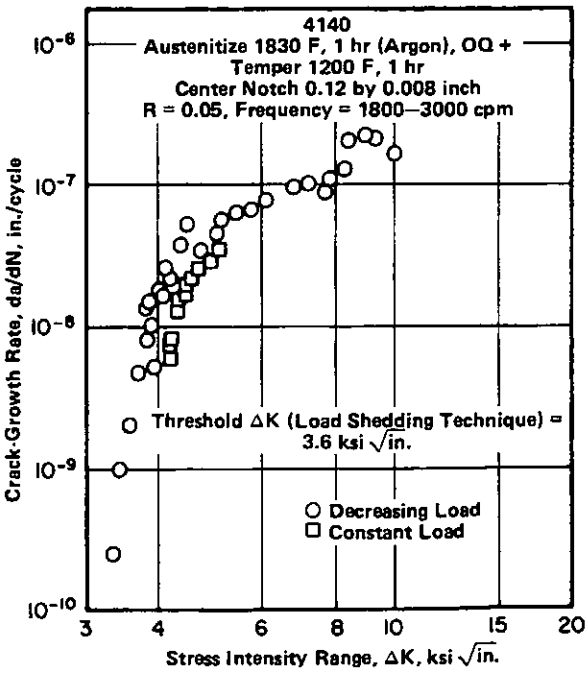

FIGURE 3.0514. ROOM TEMPERATURE FATIGUE CRACK-GROWTH BEHAVIOR OF QUENCHED AND TEMPERED 4140 STEEL AT LOW STRESSES (69)

	Fe
0.4	Cr
1	Cr
0.2	Mo

4140

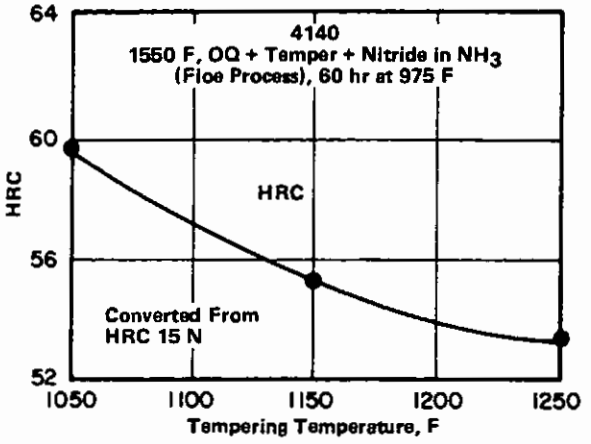

FIGURE 4.0421. CASE HARDNESS OF ALLOY NITRIDED AFTER IT HAD BEEN QUENCHED AND TEMPERED AT VARIOUS TEMPERATURES (41)

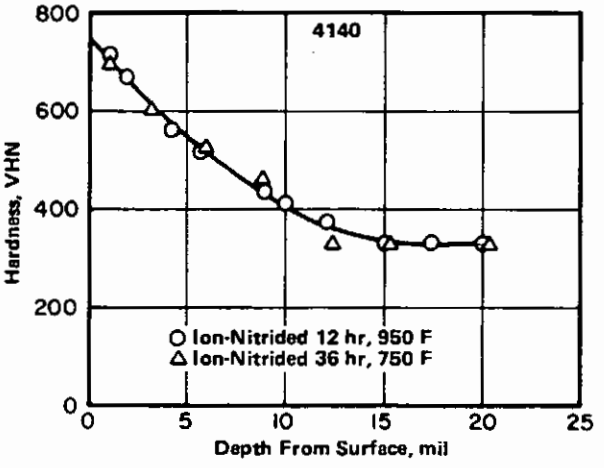

FIGURE 4.0422. HARDNESS GRADIENT NEAR SURFACE OF ION-NITRIDED 4140 STEEL (56)